ROTOR BEARING AND SHAFT DYNAMICS REDESIGN OF A DOUBLE-OVERHUNG TURBOEXPANDER FOR RELIABILITY IMPROVEMENT

by

Thomas R. Davidson

Area Maintenance Section Leader

Hoechst Celanese Chemical Corporation

Houston, Texas

Dana J. Salamone

President and Chief Engineer

Salamone Turbo Engineering, Inc.

Houston, Texas

and

Edgar J. Gunter

Professor, Mechanical and Aerospace Engineering

University of Virginia

Charlottesville, Virginia

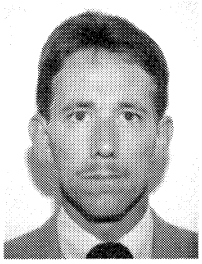

Thomas R. (Tom) Davidson is Area Maintenance Section Leader for Hoechst Celanese Chemical Group, in the Clear Lake, Texas, plant. Prior to his current position, Mr. Davidson worked for 11 years in the Maintenance Engineering Department as a Rotating Equipment Engineer. His responsibilities included technical support for troubleshooting and repairs for all types of rotating equipment, reliability improvement, vibration analysis, and new equipment review and specification.

Mr. Davidson received a B.S. degree in Mechanical Engineering from the University of Houston (1978). He is a member of IMI, ASME, and the Vibration Institute.

Dana J. Salamone received a B.S. (Mechanical Engineering) degree (1974) and an M.S. (Applied Mechanics) degree (1977) from the University of Virginia. He holds an M.B.A. degree (1984) from Houston Baptist University.

Mr. Salamone spent three years at Babcock and Wilcox, where his responsibilities included seismic structural design, stress analysis, and rotordynamics design. He was a Project Engineer at Allis Chalmers, responsible for rotordynamics and three dimensional finite element analysis of multistage centrifugal compressors. He then spent five years as Chief Engineer at Centritech Corporation, where he was responsible for rotordynamics analysis and bearing design for turbomachinery vibration problems.

In 1984, Mr. Salamone founded Turbo Engineering, Inc., for providing turnkey solutions to turbomachinery problems. He provides services in rotor bearing dynamics and finite element analysis. He also provides complete bearing, seal and coupling hardware, retrofit solutions, and repair.

Edgar J. Gunter is a Professor of Mechanical and Aerospace Engineering at the University of Virginia. He received his undergraduate degree in Mechanical Engineering from Duke University and his Masters and Ph.D. degrees from the University of Pennsylvania.

Prior to his present position, he was a Centrifugal Compressor Design Engineer with Dresser-Clark for four years and a Senior Research Engineer in the Friction and Lubrication Laboratories of the Franklin Institute. Dr. Gunter has over 30 years' experience in the rotating machinery field. He has written over 150 technical papers and reports on various aspects of the dynamics of rotating machinery and balancing.

His experience with pumps includes the dynamic analysis and experimental evaluation of the high pressure hydrogen and oxygen pumps for the space shuttle engine. Also, he has had extensive experience with various types of vertical main recirculation pumps.

ABSTRACT

A solution is presented for a lateral rotor and bearing dynamics problem on a high pressure, double-overhung turboexpander with a design operating speed of 57,300 rpm. The rotor has an expander impeller mounted at one end and a compressor impeller mounted at the other end. This unit had a long history of failures at the expander-end radial bearing. It was suspected that the frequent expander upsets were caused by unbalance degradation due to solid particle erosion on the aluminum expander-end impeller. The rotordynamics analysis of the expander with the original three lobe journal bearings predicted a high unbalance sensitivity at the expander-end of the rotor and a low logarithmic decrement for the third backward whirl mode near the design operating speed. The concern was that this mode might be excited by an unbalance-initiated rub. The redesign analysis consisted of two phases. The purpose of Phase One was to determine the best bearing redesign that could be "directly substituted" for the original bearings

without modifying the shaft or the bearing housing fit diameters and fit lengths. As a backup contingency plan, the Phase Two analysis was pursued while the Phase One retrofit was in operation. The purpose of Phase Two was to find the optimal redesign configuration that would even further improve upon the predicted Phase One retrofit achievements, without the "direct bearing substitution constraint." This option would include the possibility of a new rotor, new bearings, and possibly a new bearing housing. All objectives were met. The Phase One retrofit ran successfully for over four and one-half years without incident.

INTRODUCTION

A solution is presented for a lateral rotor and bearing dynamics problem on a high pressure, double-overhung turboexpander originally supported in a pair of three lobed, fixed geometry journal bearings. This rotor has an expander impeller mounted at one end and a compressor impeller mounted at the other end. Design operating speed is 57,300 rpm. This unit had a long history of failures at the expander-end radial bearing. It was suspected that the frequent expander upsets were caused by unbalance degradation due to solid particle erosion on the aluminum expander-end impeller. The rotordynamics analysis of the expander with the original bearings predicted a high unbalance sensitivity at the expander-end impeller. The stability analysis also predicted that the third backward whirl mode, which was very close to design operating speed, had a very low rotor stability logarithmic decrement (log dec). The concern was that this mode might be excited by an unbalance-initiated rub.

The redesign analysis consisted of two phases described as follows:

- Phase One. The purpose of Phase One was to determine the best bearing redesign that could be "directly-substituted" for the original bearings without requiring major modifications to the shaft or the bearing housing. This direct bearing substitution requirement is often referred to as the "roll-in bearing" constraint because under these conditions, the new bearings must "roll into" the bearing housing with the same outside fit diameters and lengths.

- Phase Two. As a backup contingency plan, the Phase Two analysis was pursued while the Phase One retrofit was in operation. The purpose of Phase Two was to consider the optimal redesign configuration that would even further improve upon the predicted Phase One retrofit achievements, without the "roll-in bearing" constraint. This option would include the possibility of a new rotor, new bearings, and possibly a new bearing housing.

BACKGROUND MAINTENANCE HISTORY

In January 1978, two cryogenic turboexpanders, a high pressure (HP) and a low pressure (LP), operating in series were commissioned in a carbon monoxide unit cold box.

Details of Expander Configurations

The turboexpander rotors have a double-overhung configuration. There is a shrouded, aluminum expander impeller mounted on one end of the shaft and an open-faced, aluminum compressor impeller mounted on the other end. The compressor section of these turboexpanders acts as a "speed-control brake." Both machines originally had solid bronze, fixed geometry bearings without babbitt in the bores or on the thrust faces. The expander-end journal bearing was a three-lobed design. The compressor-end bearing was a combination of a three-lobed radial journal bearing and a tapered-land thrust bearing. The design operating speeds are 57,300 rpm for the HP expander and 38,200 rpm for the LP expander. Both the HP and LP expanders were originally equipped with "X" and "Y" proximity probes and shaft vibration was continuously monitored. It is important to note that the expander manufacturer located these probes near the center of the rotor. However, this is not the position where maximum amplitudes occur on an overhung rotor. This factor has to be taken into account when addressing the magnitudes of the field vibration levels.

Failures of Original Bearings

Historically, when the expanders were in "good condition," the unfiltered vibration levels were in a range between 0.3 and 0.5 mils. Mechanical and/or electrical runout typically accounted for 0.12 to 0.25 mils of these overall vibration levels. Therefore, it is reasonable to conclude that these expanders could operate with very acceptable vibration levels, under optimum conditions.

During the first three years of operation, there were four bearing failures on the HP expander and two bearing failures on the LP expander. In all six instances, the failure occurred at the expander-end radial bearing. After a bearing failure occurred, the unfiltered vibration levels would increase to a level ranging between 2.5 and 3.0 mils. A review of the vibration spectra, after a bearing failure, indicated a significant level of broad-band subsynchronous vibration that ranged from 25 to 35 percent of the operating speed. In addition, there was a significant increase in the synchronous vibration amplitude. After these episodes, the inspection of the bearing bore repeatedly revealed that the bearing "wiping" had occurred opposite the direction of rotation. This backward wiping mechanism was a phenomenon that initially was not understood.

In addition to the previously stated problems, it was not possible to successfully operate the HP expander at design operating speed due to high expander-end radial bearing temperatures and shaft vibration instabilities. This problem persisted even after several correction attempts were made.

The early failures were attributed to improper startup and operation. However, subsequent follow up investigations never revealed any significant operational or process upsets other than minor system pressure and temperature variations. It therefore became obvious that these machines were very sensitive to minor process excursions. An effort was made to better define startup procedures and to improve process-instrument controls in order to minimize operational excursions. After the improved procedures and controls were established, the machines ran without a bearing failure for two years. However, the HP expander was still operating below design speed.

Gas Stream Contamination and Impeller Erosion

In late 1982, problems surfaced with contamination in the expander-end process gas stream. A lengthy investigation revealed that the contamination consisted of solid particles that were introduced from an upstream process vessel. The solid particles entering the HP expander inlet were eroding the periphery of the expander-end impeller. This erosion caused degradation of the balance condition as a function of time. This degradation was confirmed by a progressive increase in the synchronous vibration amplitudes monitored at the vibration probes near the center of the rotor. When the vibration amplitudes would reach 1.0 to 1.5 mils, the operating unit was shut down and the expander was replaced with a complete spare expander cartridge. There were numerous occasions when the HP expander would experience a bearing wipe before it was possible to make a planned unit shutdown. Documentation shows that this erosion-induced balance degradation contributed to ten bearing failures within a two-year period. All of these bearing failures occurred at the expander-end radial bearing. In addition, there were seven other outages that resulted in expander-end damage which were directly related to gas stream contamination.

Dual Path Solution Approach

There were significant production losses due to these unpredictable failures. The magnitude of the financial losses due to the outages justified a dual path solution approach, as outlined below:

- Path One. The first path addressed the expander-end process stream contamination problem. Specifically, this path consisted of the installation of a better upstream filtration system to the expander cold box. The original filter design consisted of large "sock-type" cloth-filter elements. This was changed to a sintered-metal type filter system with a five-micron absolute rating.
- Path Two. The second path was to perform a rotordynamics analysis that would identify and correct any inherent problems with the existing rotor bearing expander system. There were two underlying reasons for doing this rotor analysis. The first was to investigate the rotor unbalance sensitivity. The second was to identify and correct the problems regarding high bearing temperatures and high shaft vibration instabilities. These problems restricted operation of the HP expander below the design running speed.

Rotordynamics Analysis of Original Rotor Bearing System

A lateral rotordynamics analysis is presented of a double-overhung, high pressure (HP) turboexpander. The first portion of this analysis focuses on the prediction of the original system dynamics. Correlation of these predictions to field observations is imperative in the solution process.

Original Rotor Bearing System Modelling

A cross section of the HP expander assembly is presented in Figure 1. The rotating element consists of a 20.1 in long shaft which supports two overhung impellers. There is a compressor impeller mounted on one end and an expander impeller mounted on the other end. Note that the compressor has an open impeller and the expander has a closed impeller. The maximum operating speed for dynamic computations was assumed to be 58,000 rpm. The entire rotating assembly weighs 24.2 lb. The rotor is mounted in two three-lobe journal bearings separated by a 11.6 in bearing span. A layout of the HP expander rotor is shown in Figure 2.

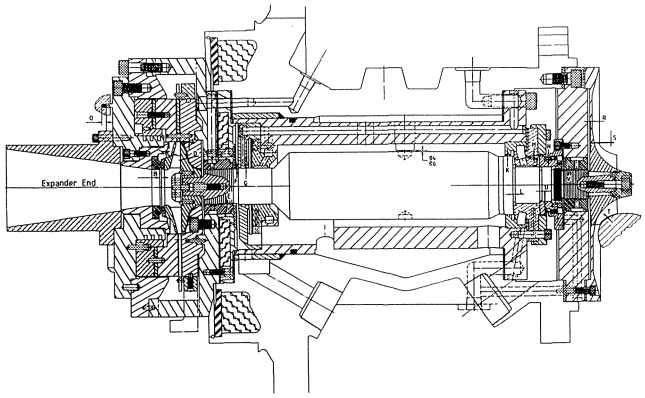

Figure 1. Cross Section of Original HP Expander Rotor and Casing.

With a high speed overhung rotor, it is important to have the accurate impeller inertias in order to properly simulate the gyroscopic and rotary inertia effects. The polar moments of inertia of both impellers were measured on an inertia table. The measured weights and inertia values were compared to the calculated values obtained from the analytical impeller models. Once there was

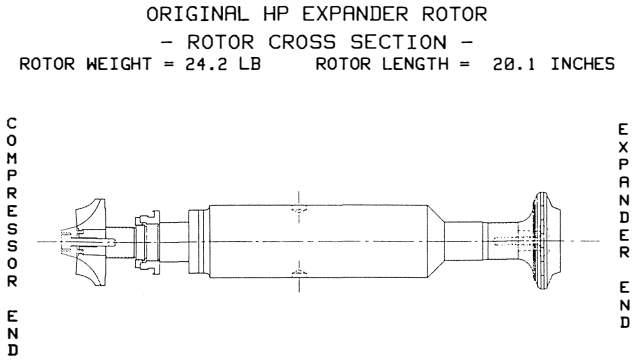

Figure 2. Original HP Expander Rotor Layout Drawing.

agreement established between measured and calculated data, the centers of gravity and transverse moments of inertia could be computed from the analytical impeller models. An outline of the computer model is depicted in Figure 3.

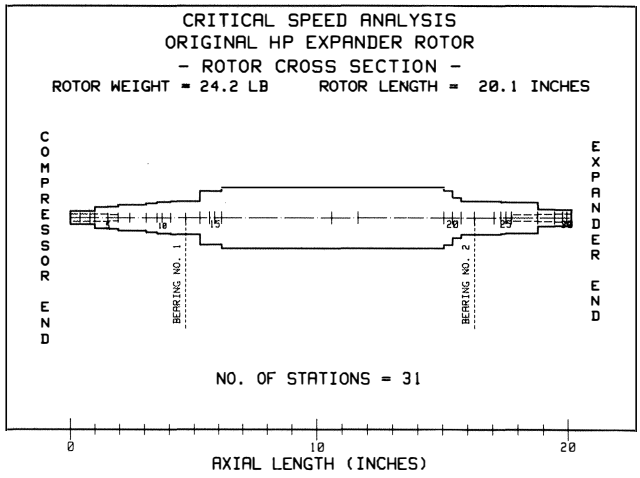

Figure 3. Original HP Expander Computer Model.

Analysis of Original Journal Bearings

The original journal bearings have a three-lobe geometry [1] similar to that shown in Figure 4. Photographs of the original compressor-end and expander-end bearings, are shown in Figures 5 and 6, respectively. Note that these bearings are made of solid bearing bronze and there is no babbitt in the bores or on the thrust bearing faces. The journal diameters on each end are 1.5728 in. The compressor-end bearing has a pad length of 0.91 in, preload of 90 percent and a diametral set clearance of 0.0022 in. The expander-end bearing has a pad length of 0.77 in, preload of 88 percent and a diametral set clearance of 0.0023 in. The bearing gravitational loads are 12.2 lb at the compressor end and 12.0 lb at the expander-end. The lubricating oil is an International Standards Organization (ISO) 32, which has a specification of 154.5 Saybolt Seconds Universal (SSU) at 100°F and 44.3 SSU at 210°F. Based upon field measurements the bearing bulk oil discharge temperature was 155°F. The absolute oil viscosity (1.346 microreyns) used in the bearing analysis was based upon this temperature. As a reference, the bearing inlet oil temperature was 110°F. Therefore, the bearing oil temperature rise was 45°F. The bulk oil discharge temperature should not be confused with the resistance temperature detector

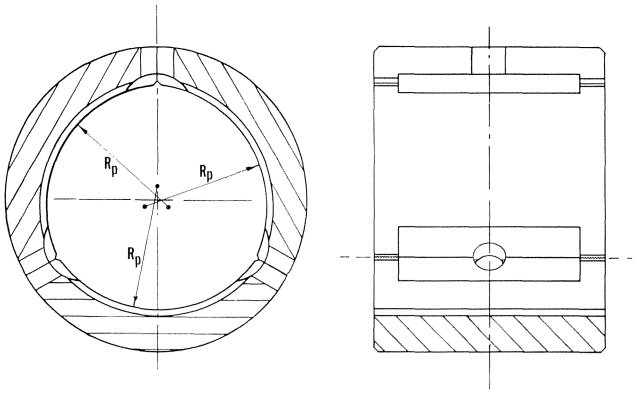

Figure 4. Typical Original Three-Lobe Journal Bearing Configuration.

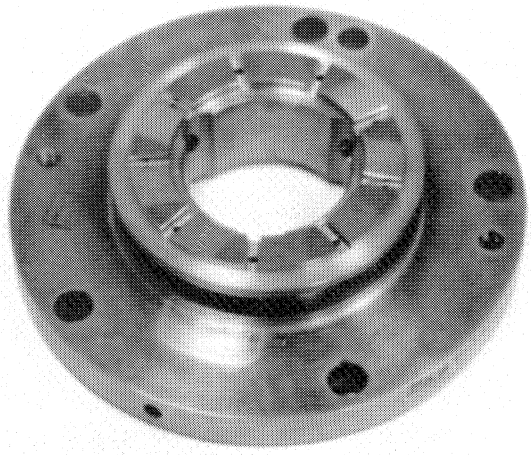

Figure 5. Photograph of Original Compressor-End Combination Tapered Land Thrust and Three-Lobe Journal Bearing.

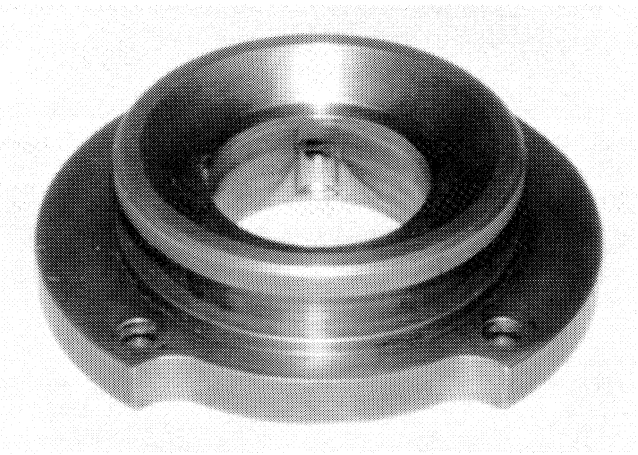

Figure 6. Photograph of Original Three-Lobe, Expander-End Journal Bearing.

(RTD) metal temperatures, which were as high as 185°F. Due to physical access constraints, these RTD temperatures were not measured at the minimum oil film thickness location so the maximum metal temperatures would be even higher than the RTD-measured values in this application. These qualifications should clarify the reasons for setting the maximum allowable bearing temperatures, measured by the RTDs, at 185°F.

The speed-dependent stiffness and damping coefficients are presented in Tables 1 and 2. The tables of bearing coefficients also list the bearing stability condition. Both bearings are stable over the operating range.

Table 1. Stiffness and Damping Coefficients for Original Three-Lobe, Compressor-End Journal Bearing.

	Speed (RPM)						
	2,000	5,000	10,000	28,000	38,000	58,000	78,000
Stiffness X 10^{-5} (lb/in)							
KXX	0.2979	0.3674	0.5888	1.5316	2.0960	3.2933	4.5759
KXY	0.1521	0.1888	0.2830	0.6711	0.9064	1.4147	1.9710
KYX	0.0097	–0.0381	–0.1313	–0.5245	–0.7647	–1.2839	–1.8518
KYY	0.2211	0.2727	0.4864	1.4234	1.9874	3.1847	4.4679
Damping X 10^{-1} (lb-sec/in)							
CXX	11.0000	6.6000	5.6800	5.5170	5.6100	5.8520	6.1170
CXY	3.0000	1.3300	0.8600	0.5300	0.4710	0.4150	0.3930
CYX	2.0000	0.5600	0.1500	–0.1960	–0.2560	–0.3410	–0.4150
CYY	8.2500	5.0000	4.4400	4.7340	4.9280	5.2670	5.5660
Stability	STABLE	STABLE	STABLE	STABLE	STABLE	STABLE	STABLE

Bearing Parameters

D=1.5728	L=0.9063 L/D=0.58	CDSET=2.2 CDSET/D=1.4	CDPAD=25 M=0.9	ISO 32 OIL MU=1.346	T-155 RHO=0.824	W-12.2 W/LD-8.6

Table 2. Stiffness and Damping Coefficients for Original Three-Lobe, Expander-End Journal Bearing.

	Speed (RPM)						
	2,000	5,000	10,000	28,000	38,000	58,000	78,000
Stiffness X 10^{-5} (lb/in)							
KXX	0.2677	0.3713	0.6352	1.7218	2.3666	3.7268	5.1752
KXY	0.1787	0.2310	0.3479	0.8188	1.1014	1.7071	2.3643
KYX	0.0149	–0.0425	–0.1578	–0.6347	–0.9230	–1.5414	–2.2121
KYY	0.2744	0.3426	0.5940	1.6700	2.3123	3.6687	5.1139
Damping X 10^{-1} (lb-sec/in)							
CXX	11.3000	7.2500	6.4700	6.4410	6.5610	6.8270	7.1040
CXY	3.8300	1.7300	1.1600	0.7330	0.6790	0.6350	0.5880
CYX	2.6100	0.8500	0.3400	–0.1120	–0.1870	–0.2690	–0.3220
CYY	10.3800	6.3500	5.5200	5.6820	5.8290	6.1180	6.4420
Stability	STABLE	STABLE	STABLE	STABLE	STABLE	STABLE	STABLE

Bearing Parameters

D=1.5728	L=0.7677 L/D=0.49	CDSET=2.3 CDSET/D=1.5	CDPAD=19.2 M=0.88	ISO 32 OIL MU=1.346	T-155 RHO=0.824	W-12.0 W/LD-9.9

Undamped Critical Speed Analysis of Original System

The critical speed map shown in Figure 7 is for the HP expander rotor with the original three-lobe journal bearing characteristics super-imposed. The first three mode shapes for assumed bearing stiffness values of 1×10^5 and 1×10^6 lb/in are depicted in Figures 8 through 13. The assumed bearing stiffness for each case is indicated at each bearing location.

Synchronous Unbalance Response Analysis of Original System

After this machine had to be shut down for high vibration, it was noted that there was shaft-to-bearing contact on the expander-end. In addition, there was evidence of solid-particle erosion on the expander-end impeller. Therefore, the analytical model was implemented in order to predict the magnitude of unbalance that

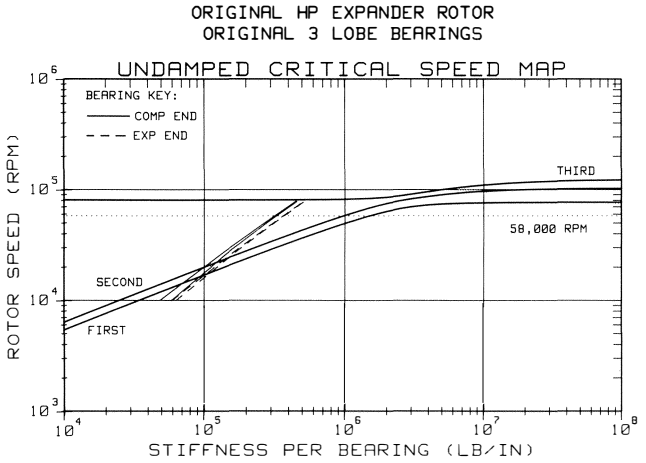

Figure 7. Critical Speed Map for Original HP Expander Rotor with Original Three-Lobe Bearing Stiffnesses Superimposed.

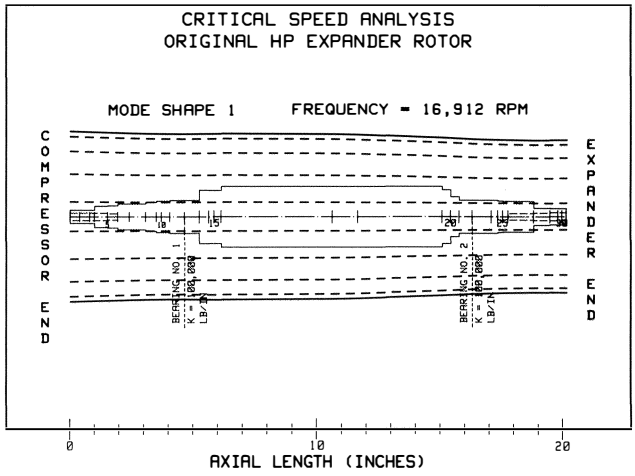

Figure 8. First Undamped Critical Speed Mode Shape for Original HP Expander Rotor. Bearing Stiffness = 100,000 lb/in. Frequency = 16,912 rpm.

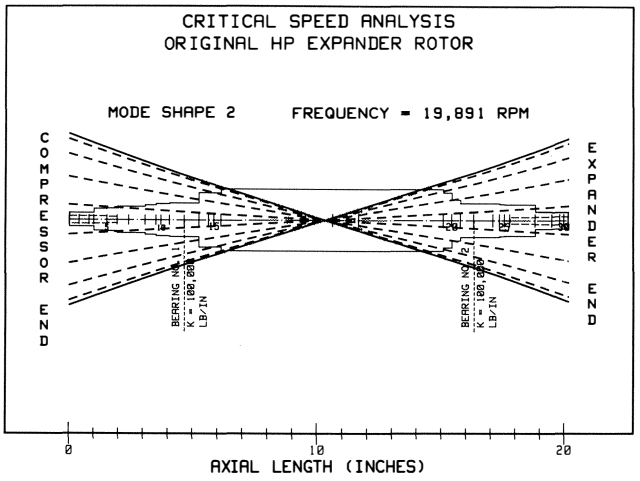

Figure 9. Second Undamped Critical Speed Mode Shape for Original HP Expander Rotor. Bearing Stiffness = 100,000 lb/in. Frequency = 19,891 rpm.

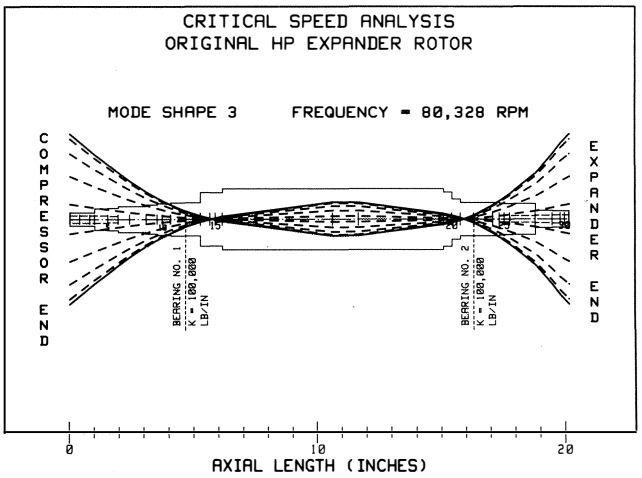

Figure 10. Third Undamped Critical Speed Mode Shape for Original HP Expander Rotor. Bearing Stiffness = 100,000 lb/in. Frequency = 80,328 rpm.

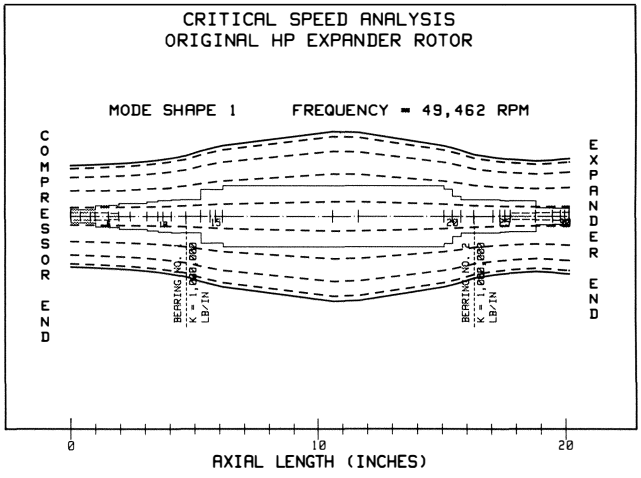

Figure 11. First Undamped Critical Speed Mode Shape for Original HP Expander Rotor. Bearing Stiffness = 1,000,000 lb/in. Frequency = 49,462 rpm.

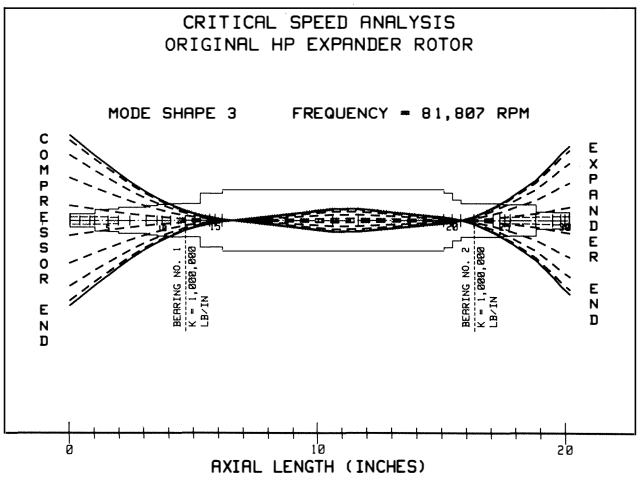

Figure 12. Second Undamped Critical Speed Mode Shape for Original HP Expander Rotor. Bearing Stiffness = 1,000,000 lb/in. Frequency = 58,413 rpm.

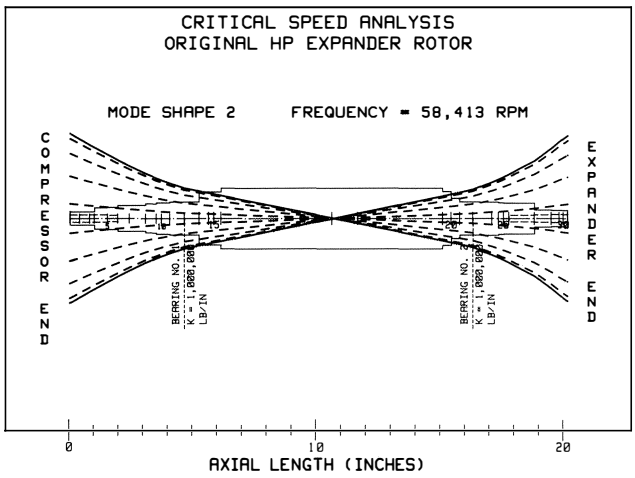

Figure 13. Third Undamped Critical Speed Mode Shape for Original HP Expander Rotor. Bearing Stiffness = 1,000,000 lb/in. Frequency = 81,807 rpm.

would cause a bearing wipe [2, 3]. Specifically, the expander-end impeller unbalance was incrementally increased in the rotordynamics model until the expander-end bearing amplitude matched the diametral bearing clearance. This amount of unbalance is referred to as the "worst case unbalance distribution." It should be noted that this is only an approximation because the linear bearing stiffness and damping coefficients were used. This assumption is acceptable for small displacements about the journal equilibrium position in each bearing. In reality, the bearing stiffness and damping coefficients become very nonlinear for large orbital displacements within the bearing. In this analysis, the intention was to determine a relative unbalance amount that would cause excessive expander-end bearing amplitudes, under the assumed conditions, and then to find a modification that would significantly improve the dynamics for the same amount of unbalance [4].

With the unbalance located only at the expander-end impeller location, the "worst case" unbalance was calculated to be 0.0732 oz-in. This amount of unbalance corresponds to an impeller eccentricity of 5.6 mils. This eccentricity is presented to give the reader a physical equivalent to relate with the level of unbalance that was used. The actual impellers did not have eccentricities anywhere near this magnitude. As previously explained, the actual source of unbalance was erosion.

A station cross reference chart presented in Table 3 is to be used in conjunction with the response tables and plots that refer to station numbers in the computer model. The rotor amplitudes are listed in Table 4 at 58,000 rpm with the "worst case" unbalance distribution assumed in this analysis. A plot of the rotor amplitudes at 58,000 rpm assuming the "worst case" unbalance distribution is depicted in Figure 14. Finally, the amplitude and polar plots at selected rotor locations are shown in Figures 15, 16, 17, 18, 19, 20, 21, and 22.

Table 3. Computer Model Stations and Locations for Original HP Expander Rotor.

Computer Model Station Number	*Location Description*
1	Compressor Shaft End
5	Impeller-Compressor End
6	Labyrinth Seal-Compressor End
12	Radial Bearing-Compressor End
18	Vibration Probe Near Rotor Center
22	Radial Bearing-Expander End
23	High Pressure Oil Seal
27	Labyrinth Seal-Expander End
29	Impeller-Seal-Expander End
31	Expander Shaft End

Table 4. Amplitudes (P-P Mils) and Phase Angles at 58,000 RPM for Original HP Expander Rotor Supported on Original Three-Lobe Journal Bearings. Unbalance at expander-end impeller only (Eccentricity = 5.6 Mils).

Station Number	*X-Amplitude (P-P Mils)*	*X-Phase (Degrees)*	*Y-Amplitude (P-P Mils)*	*Y-Phase (Degrees)*
1	6.3	344	6.2	346
2	5.8	344	5.8	346
3	5.3	344	5.3	345
4	5.1	344	5.0	345
5	4.5	344	4.5	345
6	4.0	344	4.0	345
7	3.5	343	3.5	345
8	2.8	343	2.8	344
9	2.4	342	2.4	343
10	2.2	342	2.2	343
11	1.9	341	1.9	342
12	1.5	339	1.5	341
13	1.1	336	1.1	337
14	0.9	332	0.9	335
15	0.8	330	0.8	332
16	0.6	326	0.6	328
17	1.4	174	1.4	175
18	1.7	172	1.7	172
19	2.2	164	2.1	166
20	2.2	164	2.1	165
21	2.1	163	2.1	164
22	2.0	160	2.0	162
23	1.7	150	1.7	153
24	1.6	145	1.5	149
25	1.5	140	1.4	144
26	1.4	134	1.3	138
27	1.3	86	1.1	86
28	2.0	50	1.8	46
29	2.6	40	2.4	36
30	2.9	37	2.7	33
31	3.2	35	3.0	31

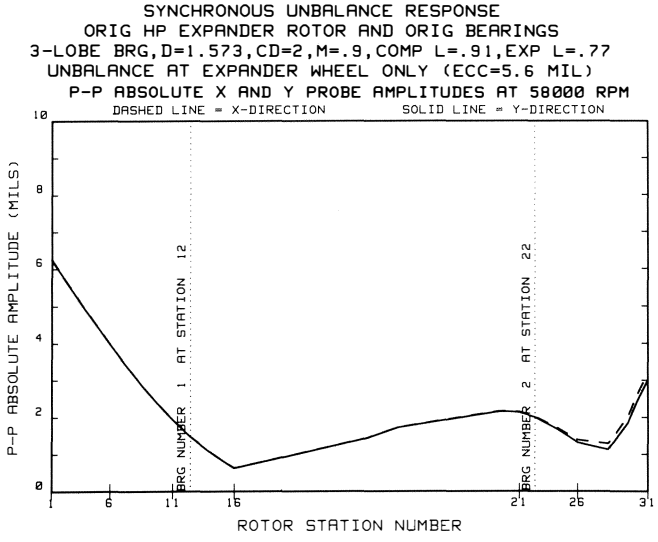

Figure 14. Magnitude of Synchronous Response Amplitude (P-P Mils) Vectors vs Rotor Station Number at 58,000 RPM for Original Rotor bearing System. Unbalance at expander-end impeller only (Eccentricity = 5.6 Mils).

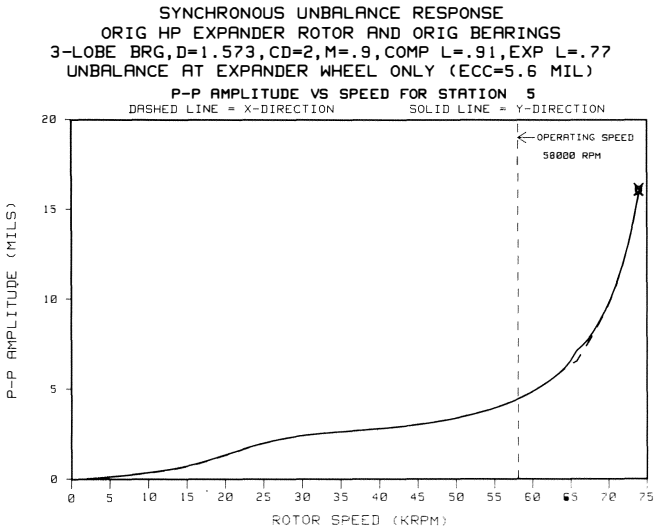

Figure 15. Synchronous Response Amplitudes (P-P) vs Rotor Speed at Compressor-End Impeller Location for Original Rotor Bearing System. Unbalance at expander-end impeller only (Eccentricity = 5.6 Mils).

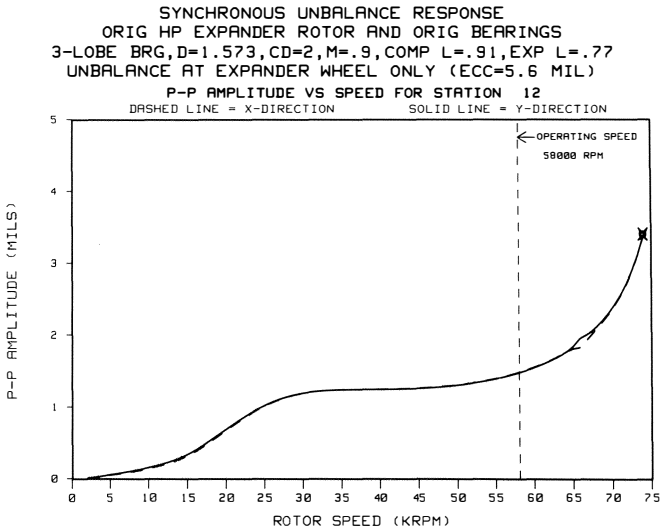

Figure 17. Synchronous Response Amplitudes (P-P Mils) vs Rotor Speed at Compressor-End Bearing Location for Original Rotor bearing System. Unbalance at expander-end impeller only (Eccentricity = 5.6 Mils).

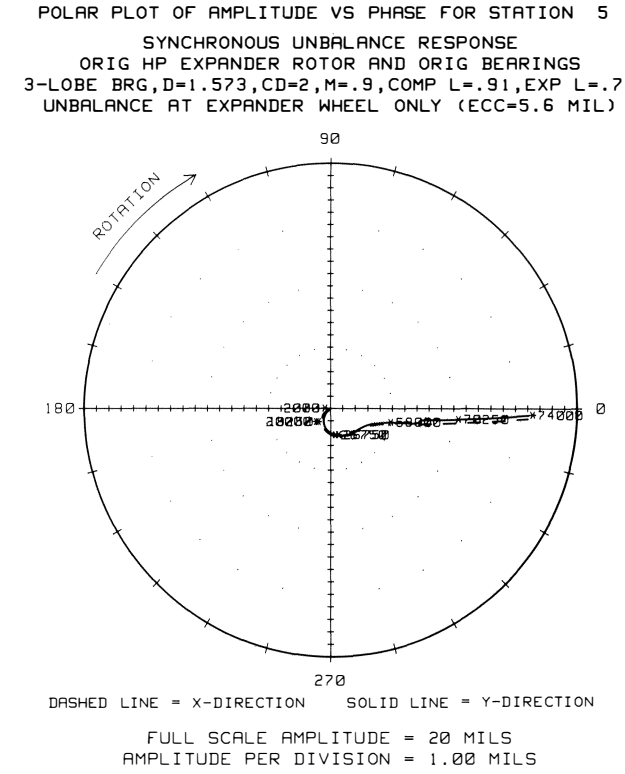

Figure 16. Synchronous Response Nyquist Plot at Compressor-End Impeller Location for Original Rotor bearing System. Unbalance at expander-end impeller only (Eccentricity = 5.6 Mils).

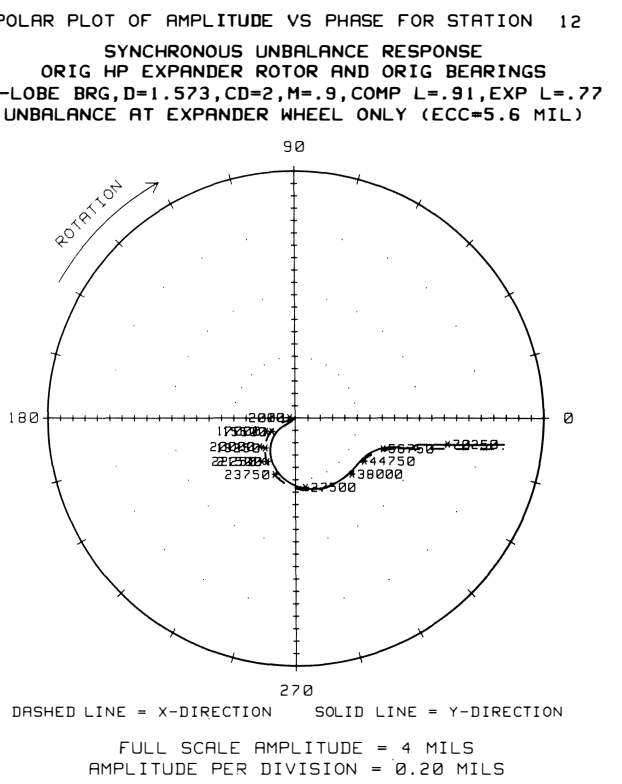

Figure 18. Synchronous Response Nyquist Plot at Compressor-End Bearing Location for Original Rotor Bearing System. Unbalance at expander-end impeller only (Eccentricity = 5.6 Mils).

Rotor Stability Analysis of Original System

The rotor stability analysis is sometimes referred to as a damped critical speed, or eigenvalue, analysis [5, 6]. The purpose of this portion of the rotordynamics study is to check for possible subsynchronous instability problems. The stability indicator is called the "logarithmic decrement." It is sometimes referred to as the "log decrement" or "log dec." This parameter is defined as the natural log of the ratio of two successive vibration amplitudes. If the log decrement is positive, the rotor system is stable. If the log decrement is negative, the rotor system is unstable. As a design criteria, it is desirable to have a log decrement greater than or equal to +0.25.

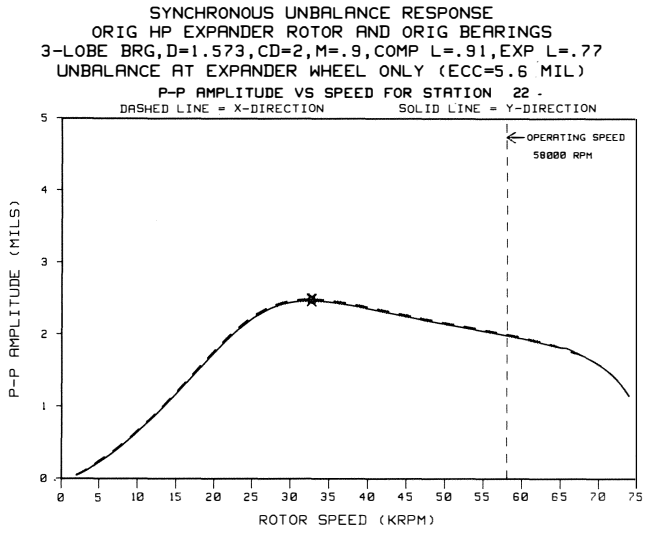

Figure 19. Synchronous Response Amplitudes (P-P Mils) vs Rotor Speed at Expander-End Bearing Location for Original Rotor Bearing System. Unbalance at expander-end impeller only (Eccentricity = 5.6 Mils).

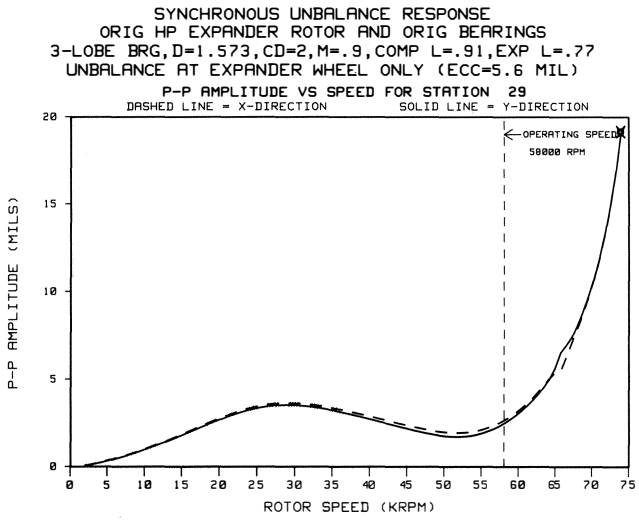

Figure 21. Synchronous Response Amplitudes (P-P Mils) vs Rotor Speed at Expander-End Impeller Location for Original Rotor Bearing System. Unbalance at expander-end impeller only (Eccentricity = 5.6 Mils).

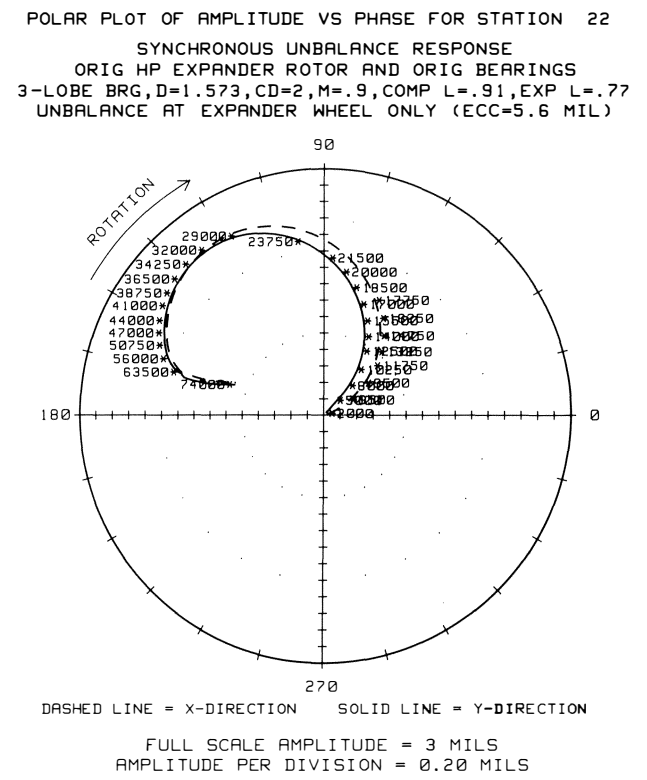

Figure 20. Synchronous Response Nyquist Plot at Expander-End Bearing Location for Original Rotor Bearing System. Unbalance at expander-end impeller only (Eccentricity = 5.6 Mils).

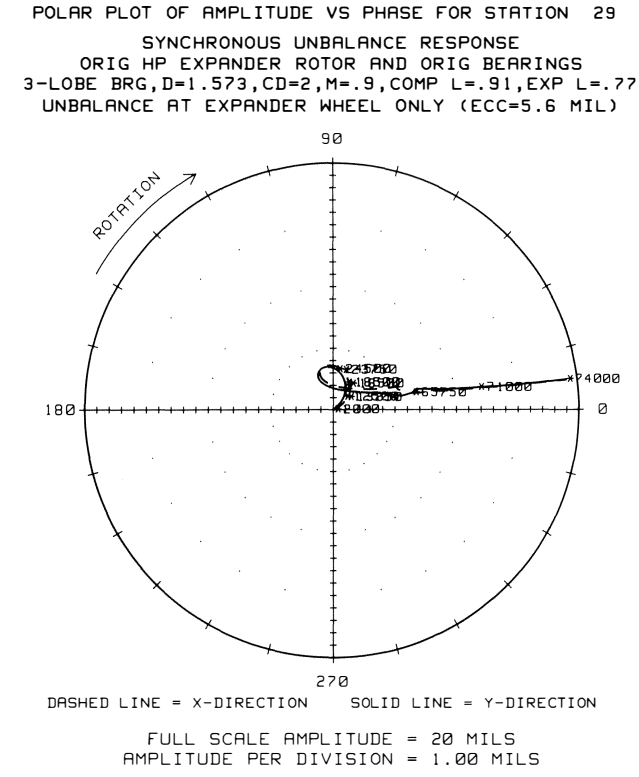

Figure 22. Synchronous Response Nyquist Plot at Expander-End Impeller Location for Original Rotor Bearing System. Unbalance at expander-end impeller only (Eccentricity = 5.6 Mils).

The stability results are listed in Table 5 for the first three forward and backward whirl modes. In particular, note the low value of the log decs of the modes with frequencies near the targeted operating speed of 58,000 rpm. These results reveal that the first and second modes are only marginally stable. The third forward mode is 79,011 rpm with a log decrement of +0.03. The third backward whirl mode is 66,880 rpm with a log decrement of only +0.07. This backward whirl mode is vulnerable to rub excitation. In addition, the close proximity of this backward mode frequency to running speed is not desirable. The mode shapes (eigenvectors) for the third backward and forward modes are illustrated in Figures 23 and 24, respectively.

Table 5. Rotor Stability Results for Original HP Expander Rotor Supported on Original Three-Lobe Journal Bearings. Operating Speed = 58,000 RPM.

Eigenvalue Number	*Damped Frequency (RPM)*	*Logarithmic Decrement (DIM)*	*Stability Condition*	*Whirl Direction*
1	30,282	+2.97	Very Stable	Backward
2	30,701	+0.39	Stable	Forward
3	34,454	+3.34	Very Stable	Backward
4	36,720	+0.70	Very Stable	Forward
5	66,880	+0.07	Marginally Stable	Backward
6	79,011	+0.03	Marginally Stable	Forward

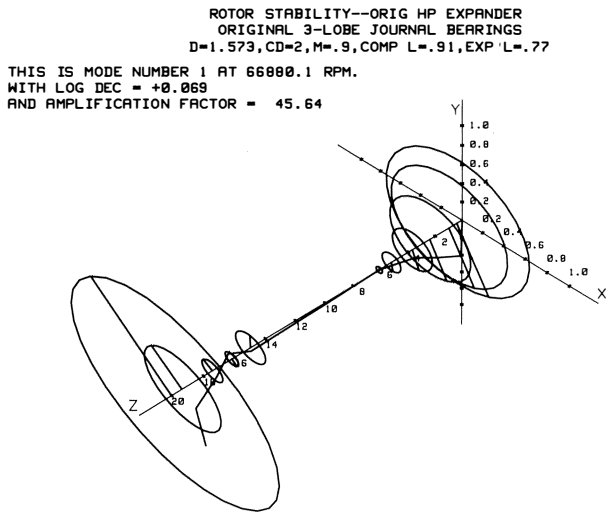

Figure 23. Third Backward Whirl Mode Shape for Original Rotor Bearing System. Operating Speed = 58,000 rpm. Damped Eigenvalue Frequency = 66,880 rpm. Log Decrement = +0.069.

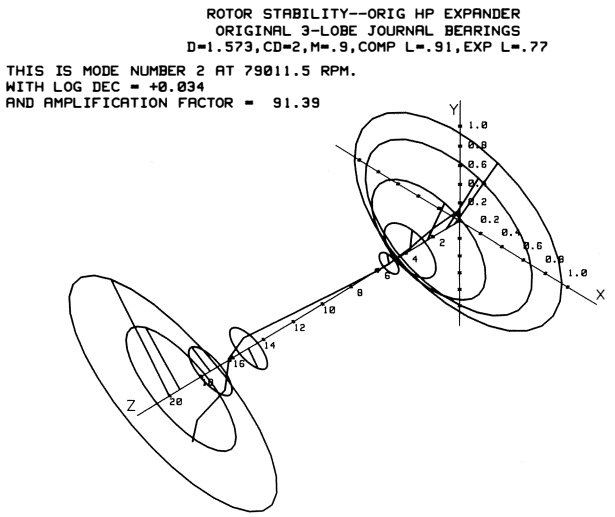

Figure 24. Third Forward Whirl Mode Shape for Original Rotor Bearing System.Operating Speed = 58,000 rpm. Damped Eigenvalue Frequency = 79,011 rpm. Log Decrement = +0.034.

The third backward mode shape is illustrated in Figure 25 with the rotor and bearings super-imposed. Note the shaft deflections through the expander-end bearing region. A "zoom" on the expander-end of the rotor is shown in Figure 26. Note that the ends of the rotor are out-of-phase.

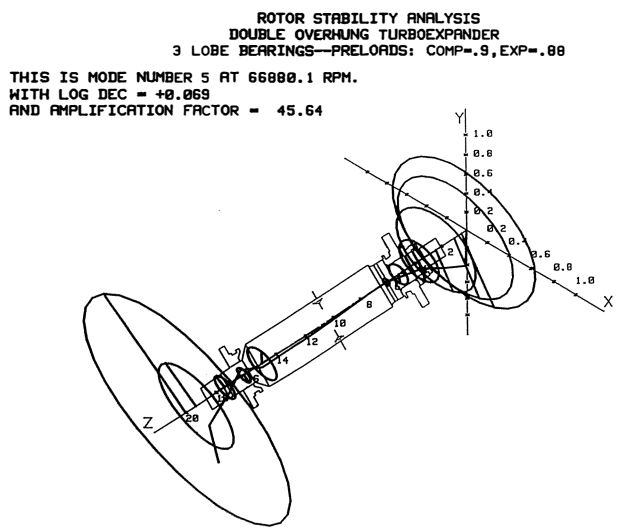

Figure 25. Superposition of Original Rotor and Bearings on Third Backward Whirl Mode Shape. Operating Speed = 58,000 rpm. Damped Eigenvalue Frequency = 66,880 rpm. Log Decrement = +0.069. Note that Expander-End of Rotor is on Left Side of Figure.

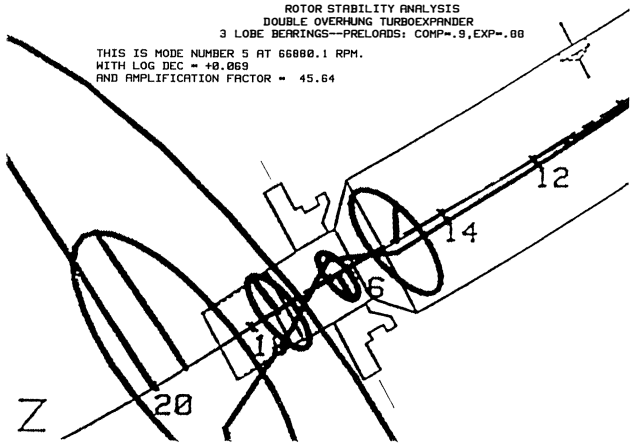

Figure 26. Zoom of Third Backward Whirl Mode Shape for Original Rotor Bearing System Focusing on the Expander-End Bearing Region. Operating Speed = 58,000 rpm. Damped Eigenvalue Frequency = 66,880 rpm. Log Decrement = +0.069.

Summary of Dynamic Characteristics for Original System

The predicted lateral rotordynamic characteristics of the HP expander in the original three-lobe journal bearings can be summarized as follows:

- The synchronous unbalance response analysis indicates that an unbalance equivalent to a 5.6 mil eccentricity at the expander-end impeller could excessively-load the expander-end bearing, which could initiate shaft-to-bearing contact. Therefore, this unbalance amount is referred to as the "worst case" assumed unbalance condition.

• The stability analysis reveals that the first and second modes are only marginally stable. The third forward mode is 79,011 rpm with a log decrement of +0.03. The third backward whirl mode is 66,880 rpm with a log decrement of only +0.07. The close proximity of this sensitive backward whirl mode frequency to the design operating speed of 57,300 rpm is not desirable, because the backward mode is particularly susceptible to rubs. Therefore, it is a significant weakness in the rotor bearing system. Specifically, it is possible that this mode might be excited by an unbalance-initiated rub.

Phase One Rotordynamics Redesign—Bearings Only

The purpose of Phase One was to determine the best bearing redesign that could be directly substituted for the original bearings without requiring modifications to the rotor or bearing housing.

Bearing Redesign—Phase One

The new journal bearings, shown in Figures 27 and 28, are a four-shoe tilting pad design with a load-between-pad orientation. These bearings have central pad pivots, preloads of 0.0 and diametral set clearances of 0.003 in. The pad lengths are 1.0 and 0.75 in at the compressor and expander-ends, respectively. The lubricating oil is the same ISO standard 32 that is currently being used in the original lube system. These bearings were designed to operate with a 30°F temperature rise. Therefore, with an inlet oil temperature of 110°F, the design bulk oil discharge temperature would be 140°F, which yields an absolute viscosity of 1.71 microreyns. This value was used to compute the Phase One bearing coefficients. The speed-dependent stiffness and damping coefficients are presented in Tables 6 and 7. The new Phase One bearing hardware is illustrated in Figures 29, 30, and 31.

Undamped Critical Speed Analysis with Phase One Bearings

The original HP expander critical speed map is shown in Figure 32 with the new Phase One tilting pad bearing stiffnesses superimposed. The Phase One retrofit assumes that the rotor is not to be modified. Therefore, the basic mode shapes are the same as previously presented for the original rotor system.

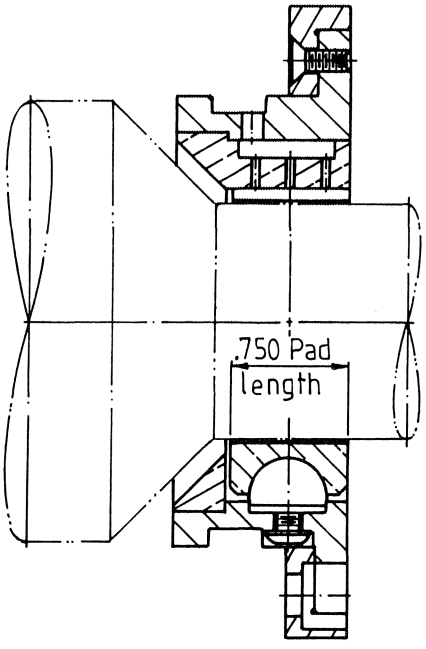

Figure 27. New Phase One Expander-End Bearing Redesign.

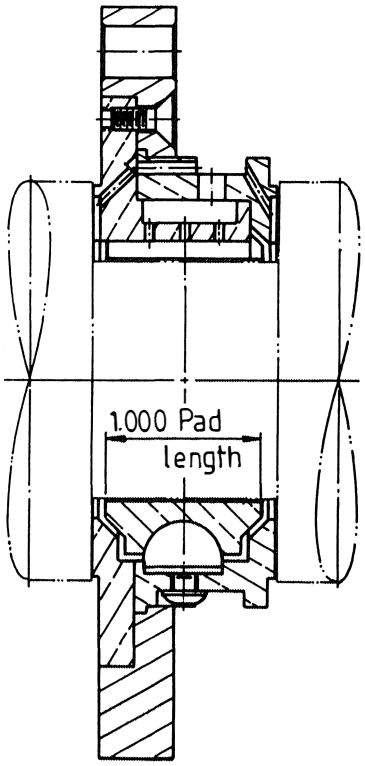

Figure 28. New Phase One Compressor-End Bearing Redesign.

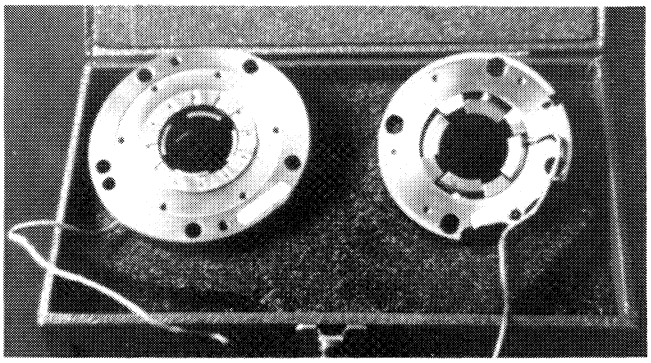

Figure 29. Photograph of Complete New Phase One Journal and Thrust Bearing Retrofit Conversion.

Table 6. Stiffness and Damping Coefficients for New Phase One, Compressor-End Tilting Pad Journal Bearing.

	Speed (RPM)						
	910	2,195	3,257	4,075	8,838	58,000	89,241
Stiffness (lb/in)							
KXX	16,886	11,123	8,916	7,691	5,240	2,396	1,997
KXY							
KYX							
KYY	16,886	11,123	8,916	7,691	5,240	2,396	1,997
Damping (lb-sec/in)							
CXX	357.0	230.8	210.1	203.6	197.3	187.7	185.8
CXY							
CYX							
CYY	357.0	230.8	210.1	203.6	197.3	187.7	185.8
Stability							

Bearing Parameters

D=1.5728	L=1.00	CDSET=3.0	CDPAD=3.0	ISO 32 OIL	T-140	W-12.2
PADARC=60	L/D=0.64	CDSET/D=1.9	M=0.0	MU=1.71		W/LD-7.8

Figure 30. Photograph of New Phase One Expander-End, Four-shoe Tilting Pad Journal Bearing Retrofit Showing Spherical Pivots.

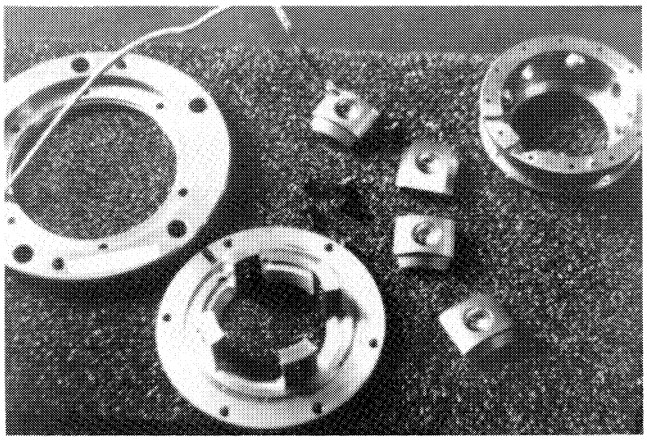

Figure 31. Photograph of New Phase One Compressor-End, Four-Shoe Tilting Pad Journal Bearing Retrofit Showing Spherical Pivots.

Table 7. Stiffness and Damping Coefficients for New Phase One, Expander-End Tilting Pad Journal Bearing.

	Speed (RPM)						
	848	2,091	4,335	9,093	14,717	58,000	90,730
Stiffness (lb/in)							
KXX	21,418	14,639	10,448	7,273	6,230	4,059	3,491
KXY							
KYX							
KYY	21,418	14,639	10,448	7,273	6,230	4,059	3,491
Damping (lb-sec/in)							
CXX	313.5	165.2	124.5	113.5	112.5	109.4	108.0
CXY							
CYX							
CYY	313.5	165.2	124.5	113.5	112.5	109.4	108.0
Stability							

Bearing Parameters

D=1.5728	L=0.75	CDSET=3.0	CDPAD=3.0	ISO 32 OIL	T-140	W-12.0
PADARC=60	L/D=0.48	CDSET/D=1.9	M=0.0	MU=1.71		W/LD-10.2

Synchronous Unbalance Response Analysis with Phase One Bearings

The unbalance criteria is the same as previously described. A comparison is shown in Table 8 of the rotor amplitudes at 58,000 rpm with the "worst case" unbalance distribution assumed in this analysis. As previously explained, the "worst case" unbalance condition considers a 5.6 mil eccentricity at the expander-end impeller. Note the improved bearing amplitudes with the new bearing design. The rotor amplitudes are listed in Table 9 at 58,000 rpm with the "worst case" unbalance distribution and a plot of these rotor amplitudes is shown in Figure 33. Finally, the amplitude and polar plots for this assumed unbalance are illustrated in Figures 34, 35, 36, 37, 38, 39, 40, and 41.

The new Phase One bearings significantly improve the unbalance response amplitudes at both bearings and at the HP oil seal, as shown in Table 8. This amplitude reduction can reduce the chances of developing a hard rub, which could set off the sensitive third backward whirl mode, as previously described in the stability analysis of the original rotor bearing system. With the original three lobe bearings, this amount of unbalance caused the expander-end bearing peak-to-peak (p-p) amplitude to match the 2.3 mil diametral clearance. The Phase One bearing redesign reduces this expander-end bearing amplitude by 47 percent. In addition, there are amplitude reductions of 44 percent at the compressor-end impeller; 45 percent at the compressor labyrinth seal; and 56 percent at the compressor-end bearing. It should be pointed out that there is a tradeoff in the form of increased amplitudes at the expander-end labyrinth and impeller. These increases are signifi-

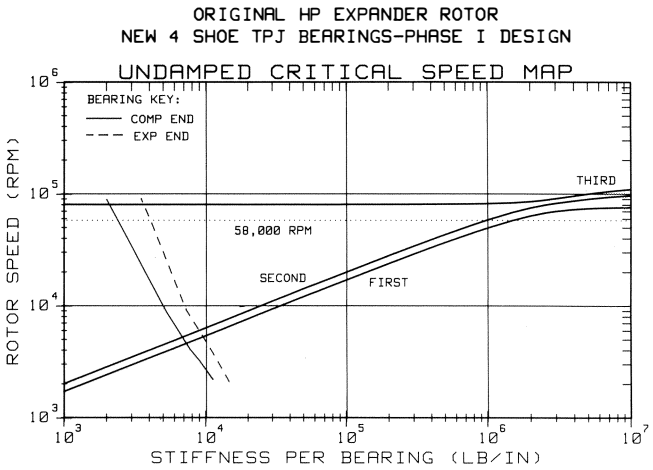

Figure 32. Critical Speed Map for Original HP Expander Rotor with New Phase One Bearing Stiffnesses Superimposed.

Table 8. Comparison of Original HP Expander Response Amplitudes (P-P Mils) at 58,000 RPM with Original and Phase One Journal Bearings. Unbalance at Expander-End Impeller Only (Eccentricity = 5.6 Mils).

	Orig Shft	*Response Original Three-Lobe Bearings*		*Response New Phase One Bearings*		*Percent Change From Original*	
Rotor Location	Sta Num	X Amp	Y Amp	X Amp	Y Amp	X Pct	Y Pct
Compr Shft End	1	6.3	6.2	3.6	3.6	–43	–42
Compr Impeller	5	4.5	4.5	2.5	2.5	–44	–44
Compr Laby	6	4.0	4.0	2.2	2.2	–45	–45
Compr Bearing	12	1.5	1.5	0.7	0.7	–56	–56
Vibration Probe	18	1.7	1.7	1.5	1.5	–13	–12
Expander Brg	22	2.0	2.0	1.1	1.1	–47	–46
HP Oil Seal	23	1.7	1.7	0.8	0.8	–55	–54
Expander Laby	27	1.3	1.1	2.3	2.3	+78	+103
Exp Impeller	29	2.6	2.5	4.7	4.7	+80	+93
Exp Shft End	31	3.2	3.0	5.5	5.5	+74	+84

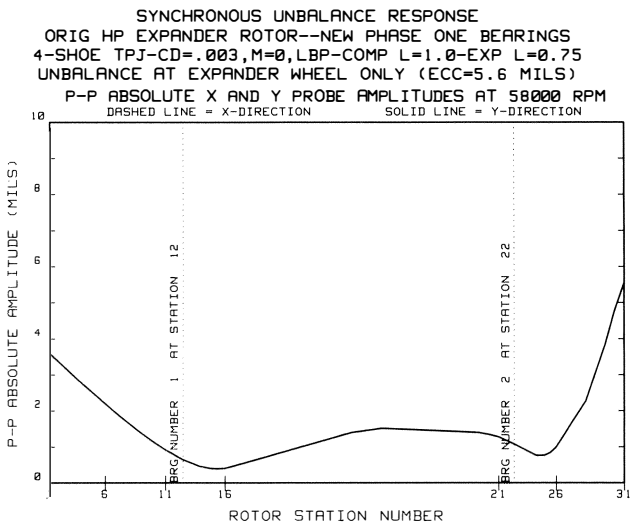

Figure 33. Magnitude of Synchronous Response Amplitude (P-P Mils) Vectors vs Rotor Station Number at 58,000 RPM for Original Rotor Supported on New Phase One Bearings. Unbalance at expander-end impeller only (Eccentricity = 5.6 Mils).

Table 9. Amplitudes (P-P Mils) and Phase Angles at 58,000 RPM for Original HP Expander Rotor Supported on New Phase One Tilting Pad Journal Bearings. Unbalance at Expander-End Impeller Only (Eccentricity = 5.6 Mils).

Station Number	X-Amplitude (P-P Mils)	X-Phase (Degrees)	Y-Amplitude (P-P Mils)	Y-Phase (Degrees)
1	3.6	335	3.6	335
2	3.3	345	3.3	345
3	3.0	334	3.0	334
4	2.9	334	2.9	334
5	2.5	333	2.5	333
6	2.2	332	2.2	332
7	1.9	331	1.9	331
8	1.5	328	1.5	328
9	1.2	325	1.2	325
10	1.1	323	1.1	323
11	0.9	320	0.9	320
12	0.6	309	0.6	309
13	0.5	287	0.5	287
14	0.4	268	0.4	268
15	0.4	256	0.4	256
16	0.4	240	0.4	240
17	1.4	177	1.4	177
18	1.5	173	1.5	173
19	1.4	160	1.4	160
20	1.3	158	1.3	158
21	1.3	155	1.3	155
22	1.1	147	1.1	147
23	0.8	110	0.8	110
24	0.8	89	0.8	89
25	0.8	73	0.8	73
26	1.0	59	1.0	59
27	2.3	29	2.3	29
28	3.8	20	3.8	20
29	4.7	18	4.7	18
30	5.1	17	5.1	17
31	5.5	16	5.5	16

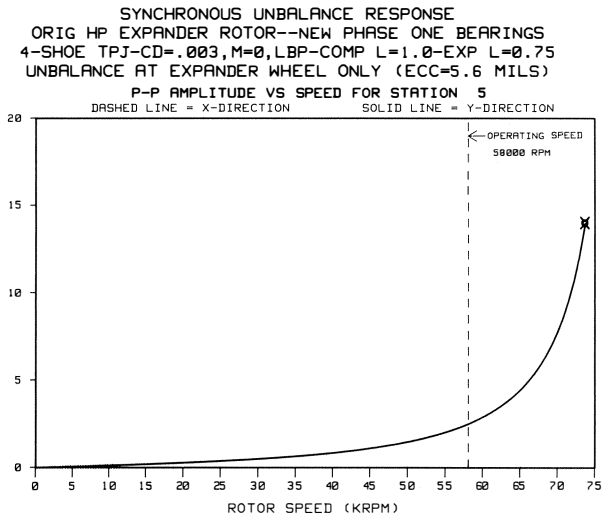

Figure 34. Synchronous Response Amplitudes (P-P Mils) vs Rotor Speed at Compressor-End Impeller Location for Original Rotor Supported on New Phase One Bearings. Unbalance at expander-end impeller only (Eccentricity = 5.6 Mils).

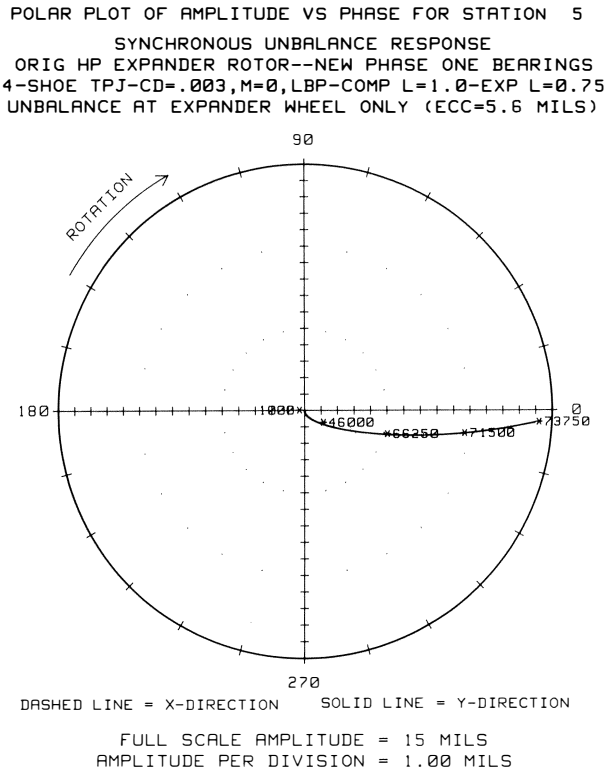

Figure 35. Synchronous Response Nyquist Plot at Compressor-End Impeller Location for Original Rotor Supported on New Phase One Bearings. Unbalance at expander-end impeller only (Eccentricity = 5.6 Mils).

cant but the end result is a more "uniform distribution" of amplitude between the ends of the rotor. For example, with the original bearings, the p-p amplitudes were 6.25 mils at the compressor-end of the shaft and 3.18 mils at the expander-end of the shaft. This represents an end-to-end amplitude ratio 1.97 to 1. With the new Phase One bearings, the p-p amplitudes are 3.59 mils at the compressor end and 5.53 mils at the expander end. In this case, the end-to-end ratio is reduced to 1.54 to 1.

Rotor Stability Analysis with Phase One Bearings

The third forward mode occurs at 78,041 rpm with a log decrement of +0.09. The third backward mode occurs at 66,121

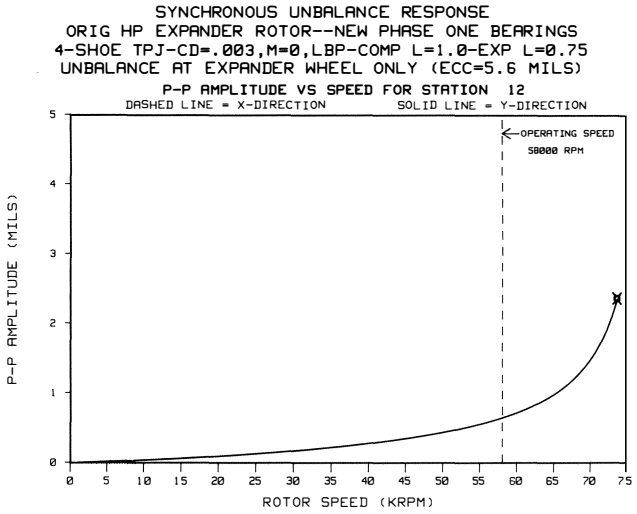

Figure 36. Synchronous Response Amplitudes (P-P Mils) vs Rotor Speed at Compressor-End Bearing Location for Original Rotor Supported on New Phase One Bearings. Unbalance at expander-end impeller only (Eccentricity = 5.6 Mils).

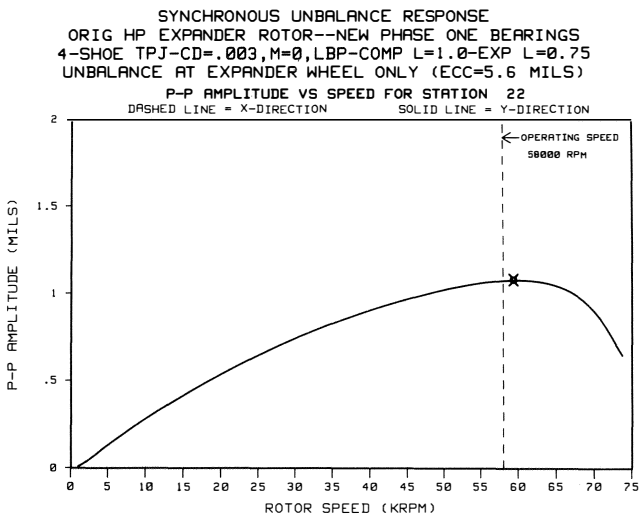

Figure 38. Synchronous Response Amplitudes (P-P Mils) vs Rotor Speed at Expander-End Bearing Location for Original Rotor Supported on New Phase One Bearings. Unbalance at expander-end impeller only (Eccentricity = 5.6 Mils).

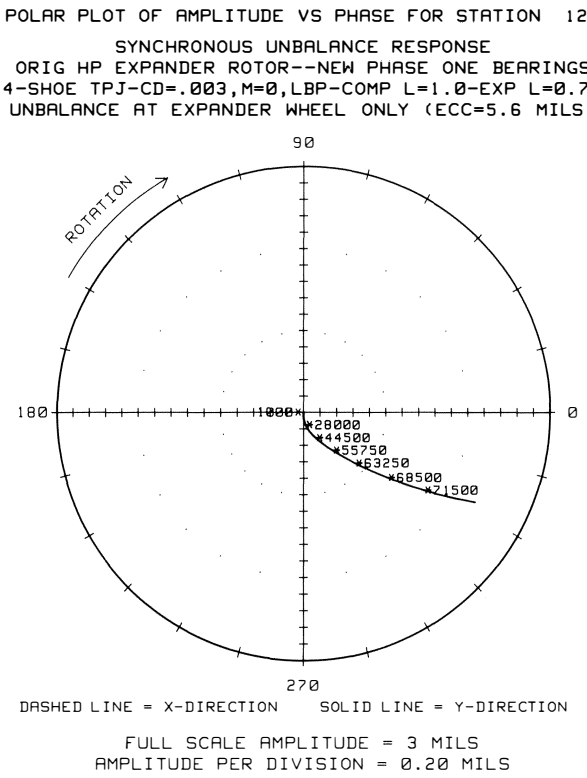

Figure 37. Synchronous Response Nyquist Plot at Compressor-End Bearing Location for Original Rotor Supported on New Phase One Bearings. Unbalance at expander-end impeller only (Eccentricity = 5.6 Mils).

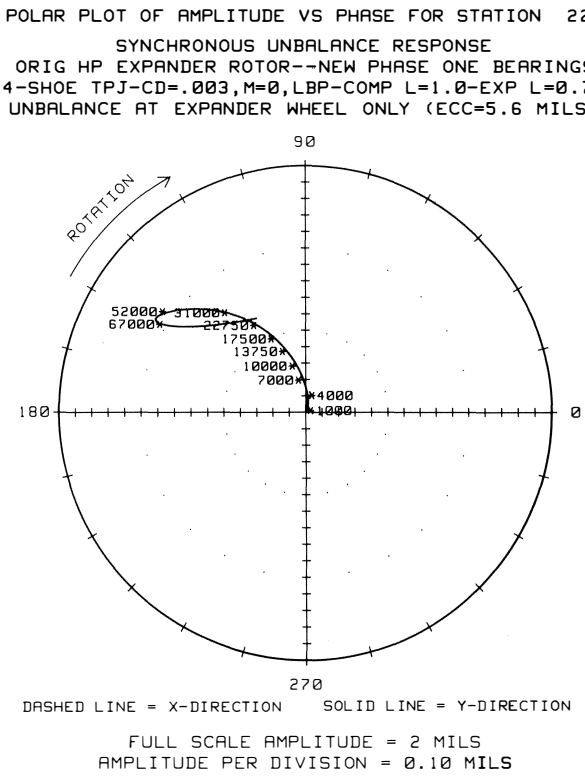

Figure 39. Synchronous Response Nyquist Plot at Expander-End Bearing Location for Original Rotor Supported on New Phase One Bearings. Unbalance at expander-end impeller only (Eccentricity = 5.6 Mils).

rpm with a log dec of +0.08. Illustrated in Figure 42 is the third backward mode with the rotor and bearings super-imposed. This mode shape shows some changes when compared to the previously shown original rotor bearing system third backward mode. For example, with the Phase One retrofit, the ends of the shaft are "in-phase." A "zoom" of the expander-end bearing region is shown in Figure 43. The stability results are listed in Table 10. The mode shapes for the two sensitive modes, discussed above, are illustrated in Figures 44 and 45.

The rotor stability condition with the new Phase One bearings is slightly improved compared to that with the original three lobe bearings. The third forward mode log dec increased from +0.03 to

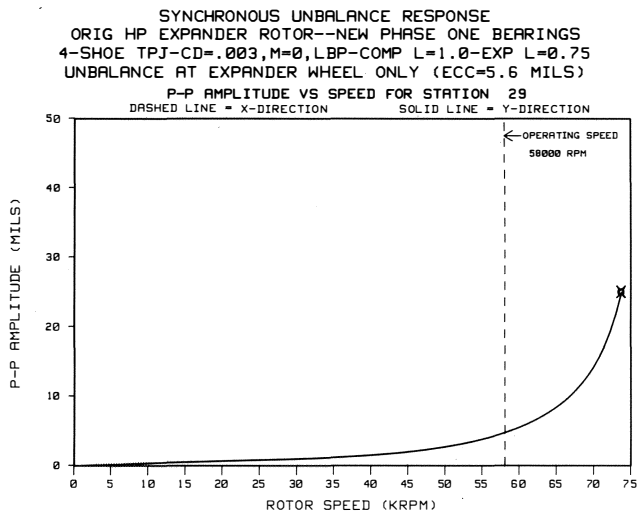

Figure 40. Synchronous Response Amplitudes (P-P Mils) vs Rotor Speed at Expander-End Impeller Location for Original Rotor Supported on New Phase One Bearings. Unbalance at expander-end impeller only (Eccentricity = 5.6 Mils).

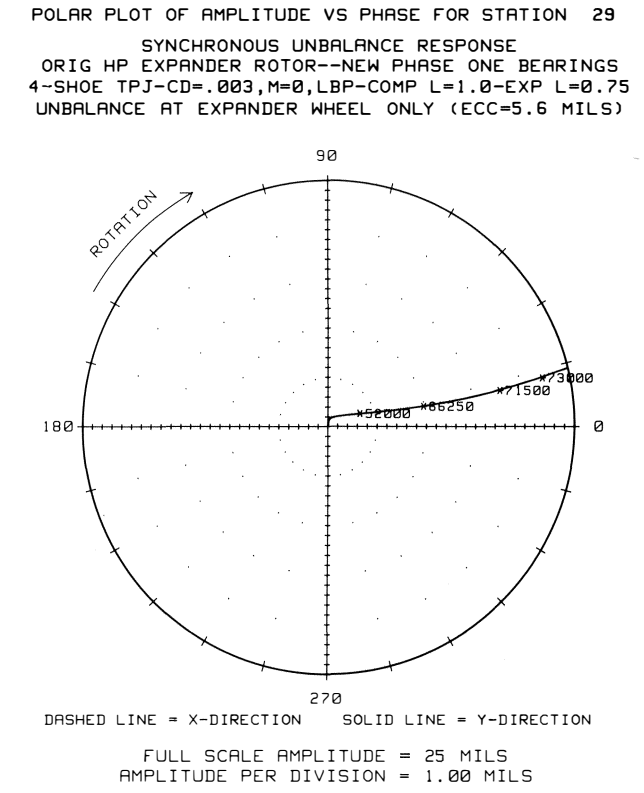

Figure 41. Synchronous Response Nyquist Plot at Expander-End Impeller Location for Original Rotor Supported on New Phase One Bearings. Unbalance at expander-end impeller only (Eccentricity = 5.6 Mils).

+0.09 and the third backward mode log dec increased from +0.07 to +0.08. However, these Phase I log decrements are still lower than desired. In addition, the third backward mode frequency decreased from 66,880 rpm to 66,121 rpm.

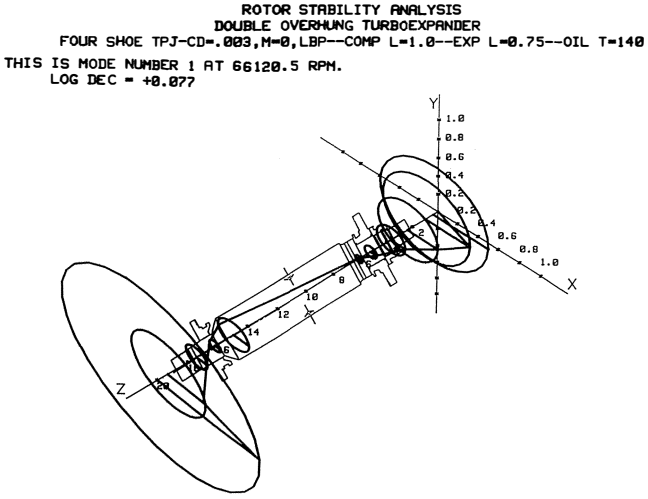

Figure 42. Superposition of Original Rotor on Third Backward Whirl Mode Shape with New Phase One Bearings. Operating Speed = 58,000 rpm. Damped Eigenvalue Frequency = 66,120 rpm. Log Decrement = +0.077. Note that expander-end of rotor is on left side of figure.

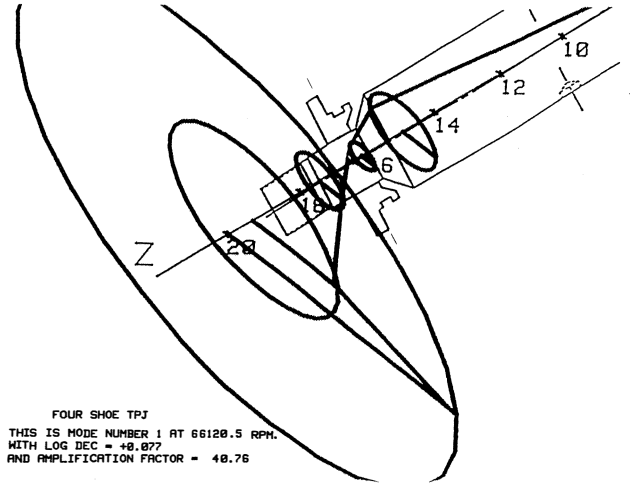

Figure 43. Zoom of Third Backward Whirl Mode Shape for Original Rotor Supported on New Phase One Bearings. Focusing on the expander-end bearing region. Operating Speed = 58,000 rpm. Damped Eigenvalue Frequency = 66,120 rpm. Log Decrement = +0.077.

Table 10. Rotor Stability Results for Original HP Expander Rotor Supported on New Phase One Tilting Pad Journal Bearings. Operating Speed = 58,000 RPM.

Eigenvalue Number	*Damped Frequency (RPM)*	*Logarithmic Decrement (DIM)*	*Stability Condition*	*Whirl Direction*
1	66,121	+0.08	Marginally Stable	Backward
2	78,041	+0.09	Marginally Stable	Forward

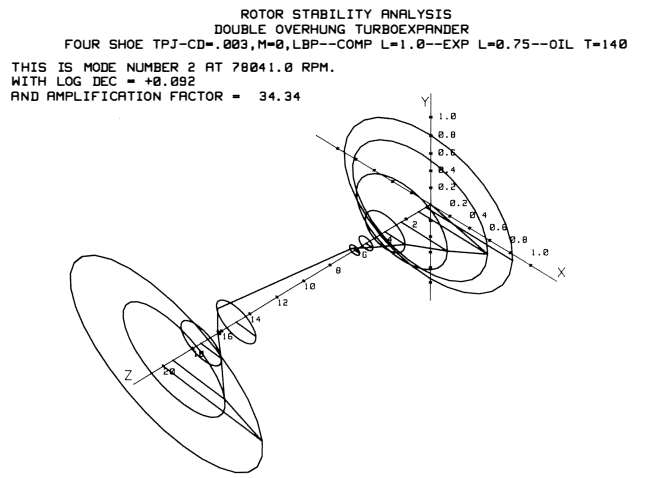

Figure 44. Third Backward Whirl Mode Shape for Original Rotor Supported on New Phase One Bearings. Operating Speed = 58,000 rpm. Damped Eigenvalue Frequency = 66,120 rpm. Log Decrement = +0.077.

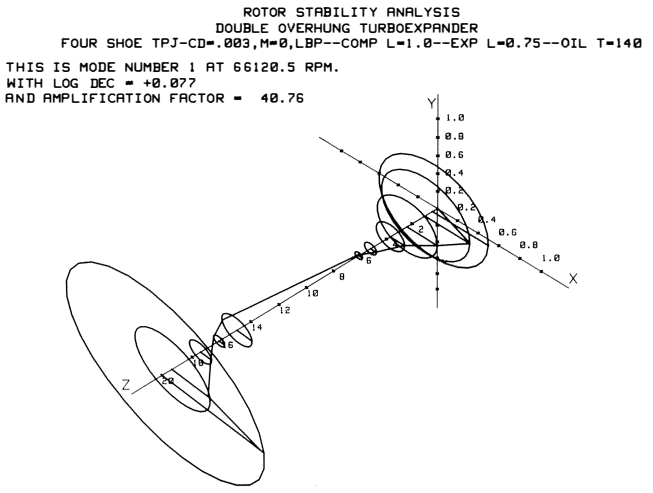

Figure 45. Third Forward Whirl Mode Shape for Original Rotor Supported on New Phase One Bearings. Operating Speed = 58,000 rpm. Damped Eigenvalue Frequency = 78,041 rpm. Log Decrement = +0.092.

Summary of Dynamic Characteristics with Phase One Bearings

The predicted lateral rotordynamic characteristics of the HP expander in the new Phase One tilt pad journal bearings can be summarized as follows:

- The new Phase One bearings significantly improve the expander unbalance response amplitudes, compared to the response with the original bearings. This amplitude reduction can reduce the chances of exciting the sensitive third backward whirl mode due to a hard rub, as discussed in the analysis of the original rotor bearing system. The worst case unbalance condition considers a 5.6 mil eccentricity at the expander-end impeller. With the original three-lobe bearings, this amount of unbalance caused the expander-end bearing peak-to-peak (p-p) amplitude to match the 2.3 mil diametral clearance. The Phase One design reduces this expander-end bearing amplitude by 47 percent.
- The rotor stability condition with the new Phase One bearings is slightly improved, compared to that with the original three-lobe bearings. However, the Phase One log decrements are still lower than desired.
- The results of this analysis have indicated that the Phase One bearing retrofit significantly improves the unbalance response of the expander rotor. It is predicted that this improvement would significantly diminish the chances of experiencing a rub due to excessive vibration amplitude. However, the Phase One retrofit does not eliminate the third backward whirl mode problem. The potential for this problem to occur could be significantly reduced by increasing the log decrement and shifting the whirl frequency further away from the operating speed. In order to meet these goals, a more extensive shaft and bearing redesign was required. This redesign will be addressed in Phase Two as a backup contingency.

FIELD RESULTS WITH PHASE ONE BEARING RETROFIT

The new Phase One journal and thrust bearings were installed in the spare HP expander cartridge in late 1986. With these new retrofit bearings, the expander started up without any major problems. During this startup, the machine was operated successfully at, and even above, the design speed of 57,300 rpm. All bearing temperatures were within design and the shaft vibration levels were less than 0.4 mils. This was the first time that the HP expander had operated at the original design speed without hot bearings and without vibration problems. These observations indicated the new Phase One bearing retrofit was a step in the right direction.

With the Phase One bearing redesign, the expanders ran very successfully for over four and one-half years without a single bearing failure. This record was documented, even though there was still some evidence of minor erosion due to solid particles in the gas stream. This success was a milestone of significant proportions. During this successful operating timeframe, there were also numerous occasions, when process and/or operational-related problems occurred, that from past experience, would have caused bearing failures with the original bearing design. On several occasions, the HP expander was unintentionally tripped on overspeed at 63,500 rpm without any detrimental effects.

As a direct result of the Phase One bearing retrofit, the mechanical reliability of the HP expander was at an all time high and was no longer a concern for plant operations. It was equally important that the increased capacity resulted from being able to reliably operate the expander at the original design speed with very low shaft vibration and normal bearing temperature levels.

While the Phase One retrofit was in operation, the Phase Two analysis contingency was carried out to completion. The Phase Two results will be presented in the following sections.

PHASE TWO ROTORDYNAMICS REDESIGN—SHAFT AND BEARINGS

As a backup contingency plan, the Phase Two analysis was pursued while Phase One retrofit was in operation. The purpose of Phase Two was to consider the optimal redesign configuration that would even further improve upon the predicted Phase One retrofit achievements, without the "roll-in bearing" constraint. This option would include the possibility of a new rotor, new bearings, and possibly a new bearing housing.

New Rotor and Bearing Redesign

The purpose of the Phase Two redesign was to identify shaft and bearing geometry changes that would improve the HP expander dynamics beyond those achieved in the Phase One redesign. The Phase One redesign was limited to bearings that would fit directly into the same physical space as the original bearings and the shaft had to remain unchanged. This analysis predicted that the unbal-

ance response was significantly improved with the Phase One bearings, but that the rotor stability log decrement was not significantly improved. Specifically, the Phase One retrofit did not eliminate the third backward whirl mode sensitivity problem. As a result of this outcome, one of the primary goals of the Phase Two analysis was to increase the log decrement of this backward whirl mode without compromising the Phase One synchronous unbalance response improvement. It was also desirable to make alterations that would shift the third backward whirl mode frequency as far as possible from operating speed.

There were four important constraints imposed on the shaft redesign:

- The tapered polygon impeller-to-shaft fits had to remain unchanged so that the existing impellers could be used.
- The labyrinth seal areas had to retain their original position and length.
- The bearing journal diameters were limited due to peripheral speed considerations.
- The outside diameter of the mid-section of the shaft was limited. This restriction was imposed because the rotor had to fit inside the bearing housing. Then the bearing housing needed to fit inside the original outer casing bore while still maintaining adequate wall thickness.

The computer model of the Phase Two shaft is illustrated in Figure 46. The shaft journal diameters were increased from 1.5728 to 2.0 in. The rotor midspan diameter was increased from 2.897 to 2.94 in. The expander-end bearing centerline was moved 0.344 in inboard and the compressor-end bearing was moved 0.625 in outboard.

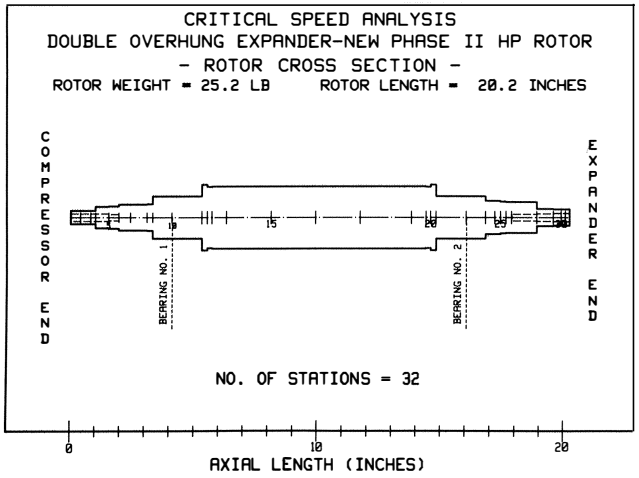

Figure 46. Phase Two HP Expander Computer Model.

Bearing Redesign-Phase Two

The new Phase Two journal bearings are a four-shoe, tilting-pad design with 2.0 in journal diameters and load-between-pad orientations. These bearings have pad lengths of 1.250 in, central pad pivots, preloads of 0.0 and diametral set clearances of 0.004 in. The lubricating oil is the same ISO standard 32 that is currently being used. These bearings were designed to operate with a 30°F temperature rise. Therefore, with an inlet oil temperature of 110°F, the design bulk oil discharge temperature would be 140°F, which yields an absolute viscosity of 1.71 microreyns. This value was used to compute the Phase Two bearing coefficients. The speed-dependent stiffness and damping coefficients are presented in Tables 11 and 12.

Table 11. Stiffness and Damping Coefficients for New Phase Two, Compressor-End Tilting Pad Journal Bearing.

	Speed (RPM)					
	859	1,721	3,065	5,092	58,000	100,000
Stiffness (lb/in)						
KXX	12,503	9,258	7,067	5,492	2,545	2,173
KXY						
KYX						
KYY	12,503	9,258	7,067	5,492	2,545	2,173
Damping (lb-sec/in)						
CXX	260.5	179.9	153.7	145.9	144.3	144.3
CXY						
CYX						
CYY	260.5	179.9	153.7	145.9	144.3	144.3
Stability						

Bearing Parameters

D=2.000	L=1.00	CDSET=4.0	CDPAD=4.0	ISO 32 OIL	T-150	W-12.0
PADARC=68	L/D=0.5	CDSET/D=2.0	M=0.0	MU=1.442		W/LD-6.0

Table 12. Stiffness and Damping Coefficients for New Phase Two, Expander-End Tilting Pad Journal Bearing.

	Speed (RPM)					
	949	1,902	3,388	5,628	58,000	100,000
Stiffness (lb/in)						
KXX	13,819	10,233	7,811	6,070	3,000	2,545
KXY						
KYX						
KYY	13,819	10,233	7,811	6,070	3,000	2,545
Damping (lb-sec/in)						
CXX	260.5	179.9	153.7	145.9	144.3	144.3
CXY						
CYX						
CYY	260.5	179.9	153.7	145.9	144.3	144.3
Stability						

Bearing Parameters

D=2.000	L=1.00	CDSET=4.0	CDPAD=4.0	ISO 32 OIL	T-150	W-12.0
PADARC=68	L/D=0.5	CDSET/D=2.0	M=0.0	MU=1.442		W/LD-6.6

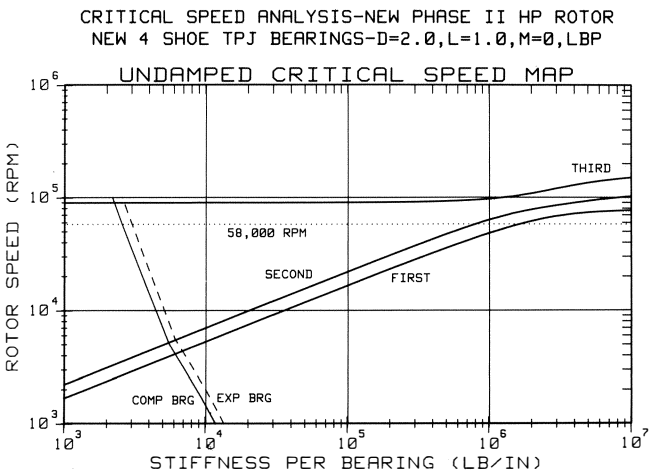

Figure 47. Critical Speed Map for Phase Two HP Expander Rotor with New Phase Two Tilting Pad Journal Bearing Stiffnesses Superimposed.

Undamped Critical Speed Analysis of Phase Two System

The critical speed map for the Phase Two rotor is shown in Figure 47. The Phase Two tilting pad journal bearing characteristics are super-imposed on the map. The first three mode shapes for

assumed bearing stiffness values of 1×10^3 and 1×10^4 lb/in are presented in Figures 48, 49, 50, 51, 52, and 53. The stiffness is indicated at each bearing location on the figures.

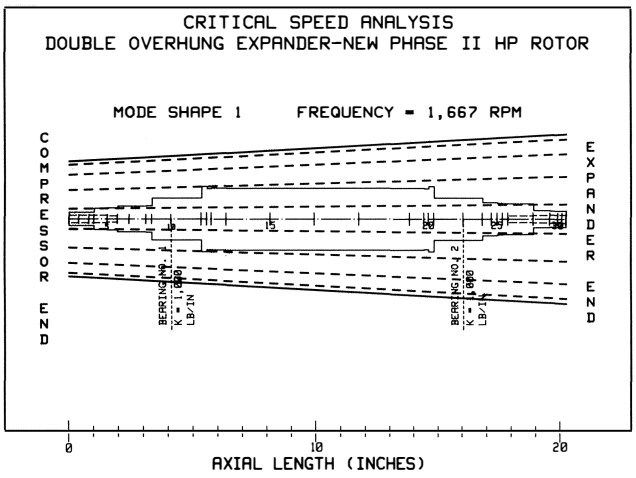

Figure 48. First Undamped Critical Speed Mode Shape for New Phase Two HP Expander Rotor. Bearing Stiffness = 1,000 lb/in. Frequency = 1,667 rpm.

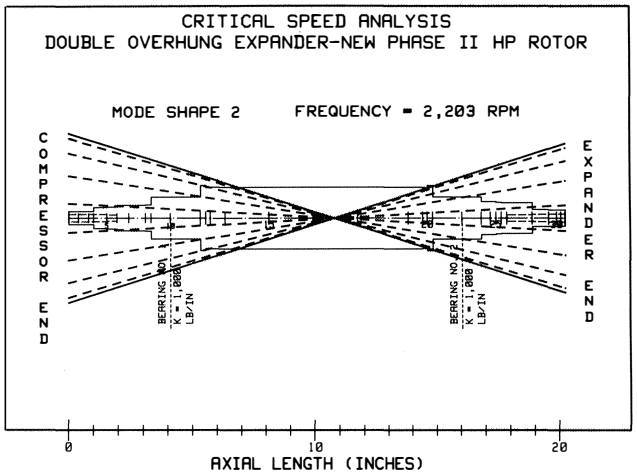

Figure 49. Second Undamped Critical Speed Mode Shape for New Phase Two HP Expander Rotor. Bearing Stiffness = 1,000 lb/in. Frequency = 2,203 rpm.

Synchronous Unbalance Response Analysis with Phase Two Bearings

A station cross-reference chart presented in Table 13 is to be used in conjunction with the response tables and plots that refer to station numbers in the computer model.

A comparison is presented in Table 14 of the rotor amplitudes at 58,000 rpm with the "worst case" unbalance distribution assumed in this analysis. The "worst case" unbalance condition considers a 5.6 mil eccentricity at the expander-end impeller. This unbalance criteria is the same as was used for the original rotor. Note the improved bearing amplitudes with the new Phase Two shaft and bearing redesign. The rotor amplitudes are listed in Table 15 at 58,000 rpm with the "worst case" unbalance distribution assumed in this analysis. A plot of these rotor amplitudes is

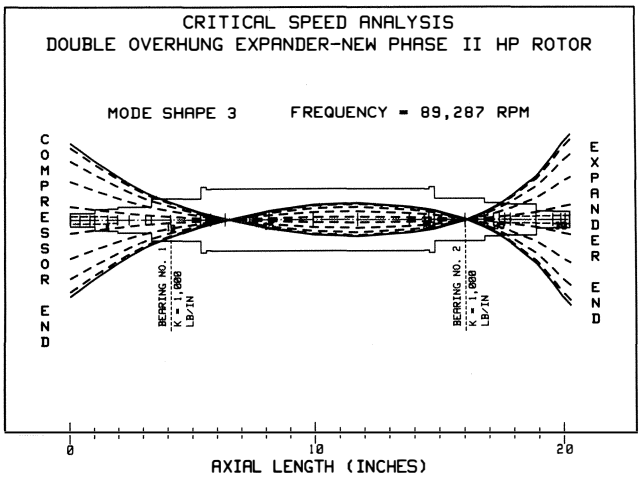

Figure 50. Third Undamped Critical Speed Mode Shape for New Phase Two HP Expander Rotor. Bearing Stiffness = 1,000 lb/in. Frequency = 89,287 rpm.

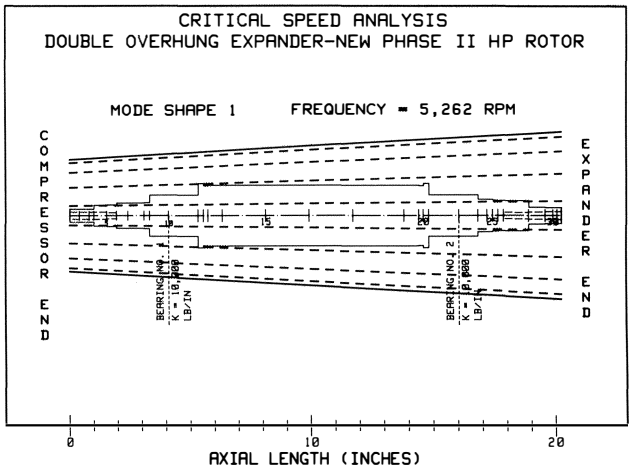

Figure 51. First Undamped Critical Speed Mode Shape for New Phase Two HP Expander Rotor. Bearing Stiffness = 10,000 lb/in. Frequency = 5,262 rpm.

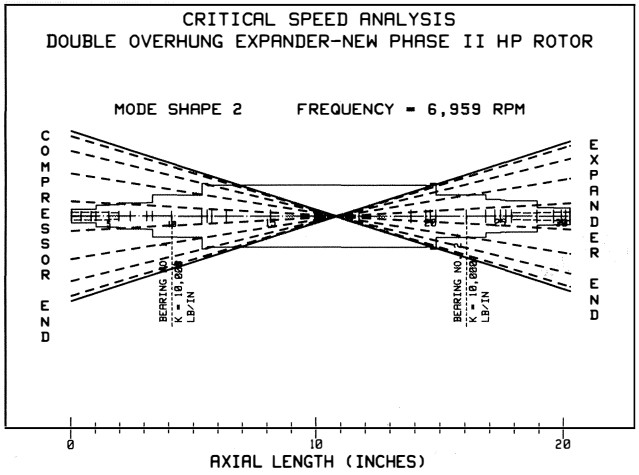

Figure 52. Second Undamped Critical Speed Mode Shape for New Phase Two HP Expander Rotor. Bearing Stiffness = 10,000 lb/in. Frequency = 6,959 rpm.

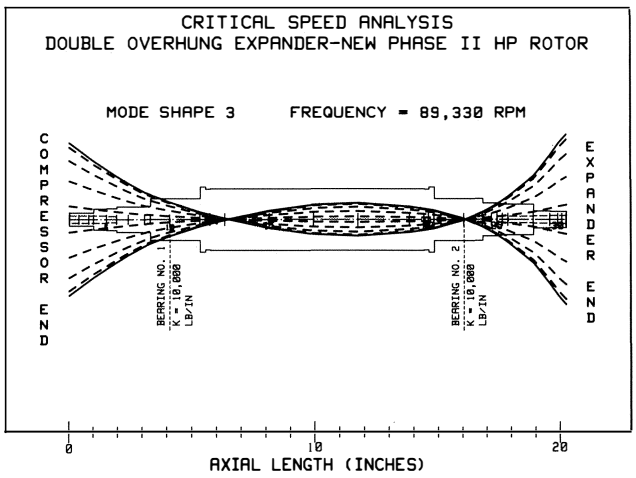

Figure 53. Third Undamped Critical Speed Mode Shape for New Phase Two HP Expander Rotor. Bearing Stiffness = 10,000 lb/in. Frequency = 89,330 rpm.

Table 13. Computer Model Stations and Locations for New Phase Two HP Expander Rotor.

Computer Model Station Number	*Location Description*
1	Compressor Shaft End
5	Impeller-Compressor End
6	Labyrinth Seal-Compressor End
10	Radial Bearing-Compressor End
17	Vibration Probe Near Rotor Center
22	Radial Bearing-Expander End
24	High Pressure Oil Seal
28	Labyrinth Seal-Expander End
30	Impeller-Expander end
32	Expander Shaft End

Table 14. Comparison of HP Expander Response Amplitudes (P-P Mils) at 58,000 RPM considering: 1) Original Rotor bearing System, 2) Original Rotor with Phase One Bearing Retrofit and 3) Phase Two Rotor bearing Retrofit. Unbalance at Expander-End Impeller Only (Eccentricity = 5.6 Mils).

	Orig Shft	*Response Original Three-Lobe Bearings*		*Response New Phase One Bearings*		*Percent Change From Original*		*Phse Two Shft*	*Response New Phase Two Bearings*		*Percent Change From Phase One*	
Rotor Location	Sta Num	X Amp	Y Amp	X Amp	Y Amp	X Pct	Y Pct	Sta Num	X Amp	Y Amp	X Pct	Y Pct
Compr Shft End	1	6.3	6.2	3.6	3.6	–43	–42	1	2.7	2.7	–24	–24
Compr Impeller	5	4.5	4.5	2.5	2.5	–44	–44	5	2.0	2.0	–20	–20
Compr Laby	6	4.0	4.0	2.2	2.2	–45	–45	6	1.8	1.8	–19	–19
Compr Bearing	12	1.5	1.5	0.7	0.7	–56	–56	10	0.9	0.9	+43	+43
Vibration Probe	18	1.7	1.7	1.5	1.5	–13	–12	17	1.2	1.2	–23	–23
Expander Brg	22	2.0	2.0	1.1	1.1	–47	–46	22	1.1	1.1	+0	+0
HP Oil Seal	23	1.7	1.7	0.8	0.8	–55	–54	24	1.0	1.0	+36	+36
Expander Laby	27	1.3	1.1	2.3	2.3	+78	+103	28	2.3	2.3	–1	–1
Exp Impeller	29	2.6	2.5	4.7	4.7	+80	+93	30	4.3	4.3	–8	–8
Exp Shft End	31	3.2	3.0	5.5	5.5	+74	+84	32	5.0	5.0	–9	–9

depicted in Figure 54. Finally, the Bodé and polar plots for this assumed unbalance are illustrated in Figures 55, 56, 57, 58, 59, 60, 61, and 62.

Refer to Table 14 for the following comparison of results. With the original three lobe bearings, the "worst case" unbalance caused the expander-end bearing peak-to-peak (p-p) amplitude to match the 2.3 mil diametral running clearance. The Phase One redesign reduced this expander-end bearing amplitude by 47 percent. The

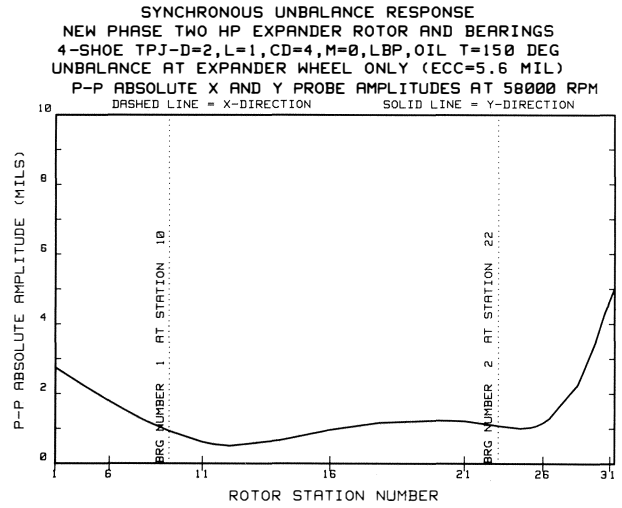

Figure 54. Magnitude of Synchronous Response Amplitude (P-P Mils) Vectors vs Rotor Station Number at 58,000 rpm for New Phase Two HP Expander Rotor Supported on New Phase Two Bearings. Unbalance at Expander-End Impeller Only (Eccentricity = 5.6 mils).

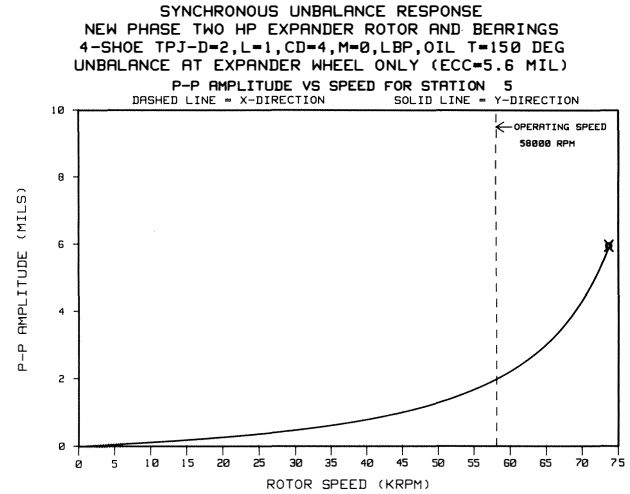

Figure 55. Synchronous Response Amplitudes (P-P Mils) vs Rotor Speed at Compressor-End Impeller Location for New Phase Two HP Expander Rotor Supported on New Phase Two Bearings. Unbalance at expander-end impeller only (Eccentricity = 5.6 mils).

Phase Two redesign results at the expander-end bearing match the Phase One results. In addition, there are amplitude reductions (compared to Phase One) of 20 percent at the compressor-end impeller; 19 percent at the compressor-end labyrinth seal; one percent at the expander-end labyrinth seal and eight percent at the expander-end impeller. It should be noted, as observed in Phase One, that there is some tradeoff in the form of increased amplitude at other locations. However, this tradeoff is acceptable, because the increased amplitudes are reasonable values. For example, Table 14 indicates that the Phase Two compressor-end bearing amplitude increases by 43 percent compared to Phase One. This increase represents a change from 0.65 to 0.93 mils p-p. This is acceptable, considering that the Phase Two bearing has diametral clearance of 4.0 mils.

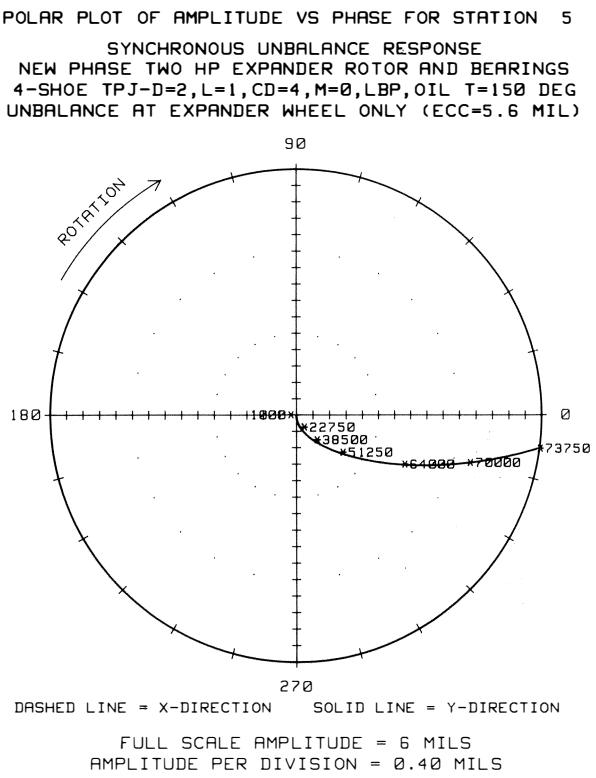

Figure 56. Synchronous Response Nyquist Plot at Compressor-End Impeller Location for New Phase Two HP Expander Rotor Supported on New Phase Two Bearings. Unbalance at expander-end impeller only (Eccentricity = 5.6 mils).

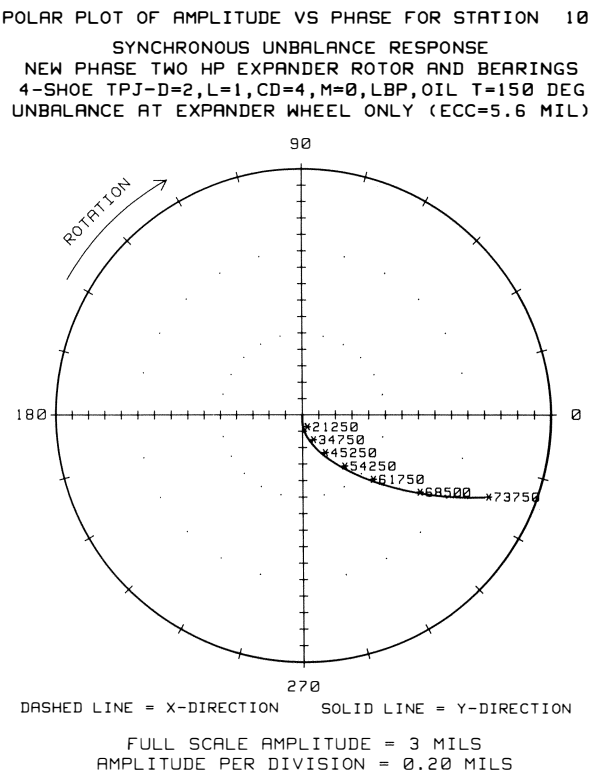

Figure 58. Synchronous Response Nyquist Plot at Compressor-End Bearing Location for New Phase Two HP Expander Rotor Supported on New Phase Two Bearings. Unbalance at expander-end impeller only (Eccentricity = 5.6 mils).

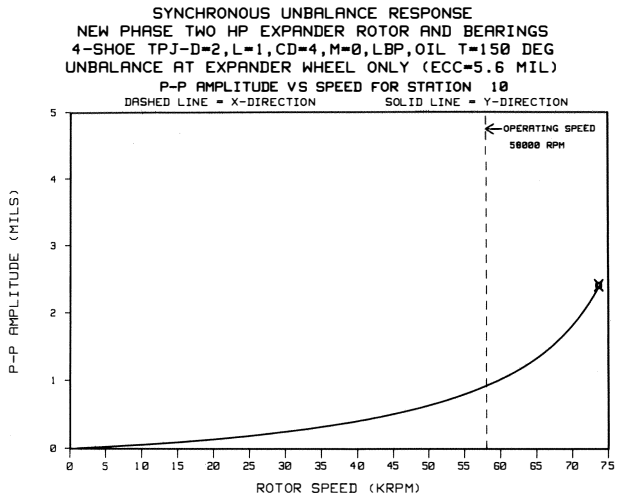

Figure 57. Synchronous Response Amplitudes (P-P Mils) vs Rotor Speed at Compressor-End Bearing Location for New Phase Two HP Expander Rotor Supported on New Phase Two Bearings. Unbalance at expander-end impeller only (Eccentricity = 5.6 mils).

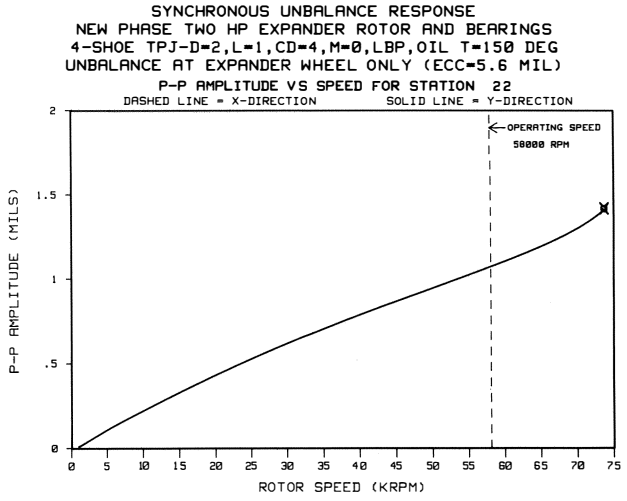

Figure 59. Synchronous Response Amplitudes (P-P Mils) vs Rotor Speed at Expander-End Bearing Location for New Phase Two HP Expander Rotor Supported on New Phase Two Bearings. Unbalance at expander-end impeller only (Eccentricity = 5.6 mils).

Rotor Stability Analysis of Phase Two System

The rotor stability analysis of the new Phase Two rotor and bearings yields a third forward mode at 84,211 rpm with a log decrement of +0.31. The third backward mode occurs at 69,562 rpm with a log dec of +0.22. The stability results are listed in Table 16. The mode shapes for the forward and backward modes discussed above are illustrated in Figures 63 and 64.

The Phase Two system significantly improves the rotor stability condition compared to the original and Phase One systems. Recall

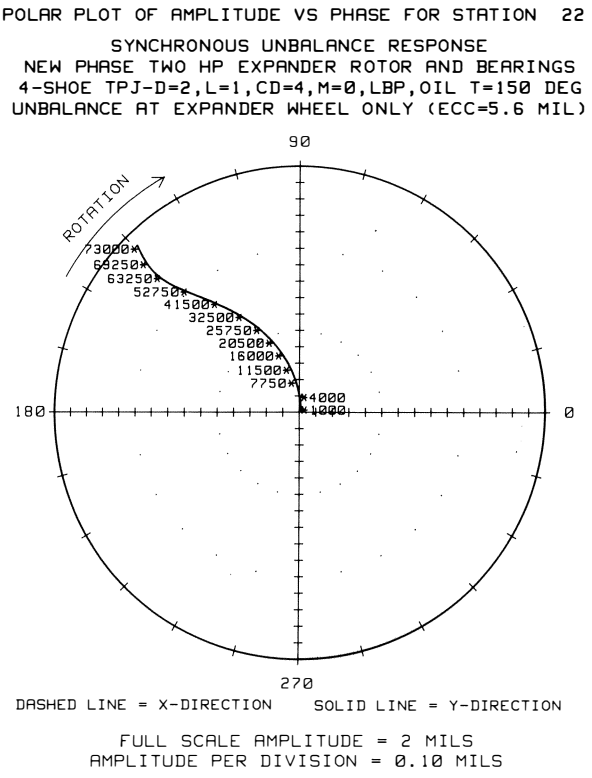

Figure 60. Synchronous Response Nyquist Plot at Expander-End Bearing Location for New Phase Two HP Expander Rotor Supported on New Phase Two Bearings. Unbalance at expander-end impeller only (Eccentricity = 5.6 mils).

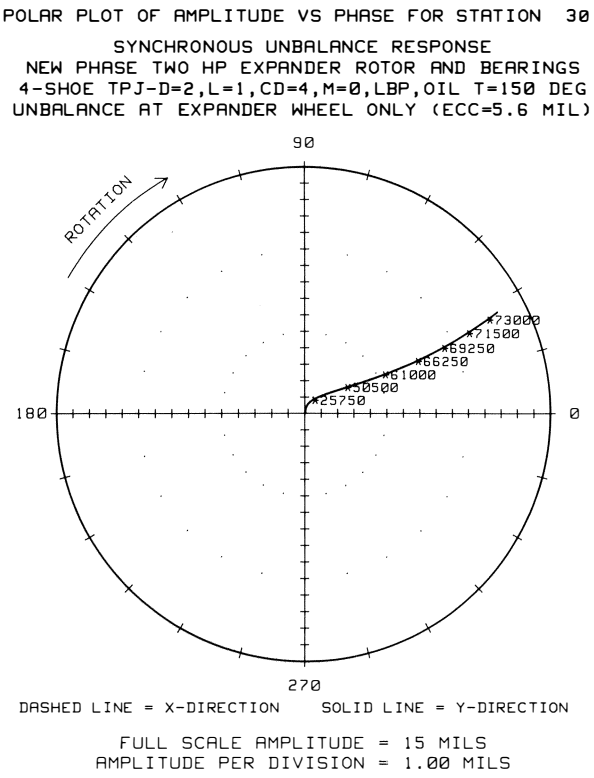

Figure 62. Synchronous Response Nyquist Plot at Expander-End Impeller Location for New Phase Two HP Expander Rotor Supported on New Phase Two Bearings. Unbalance at expander-end impeller only (Eccentricity = 5.6 mils).

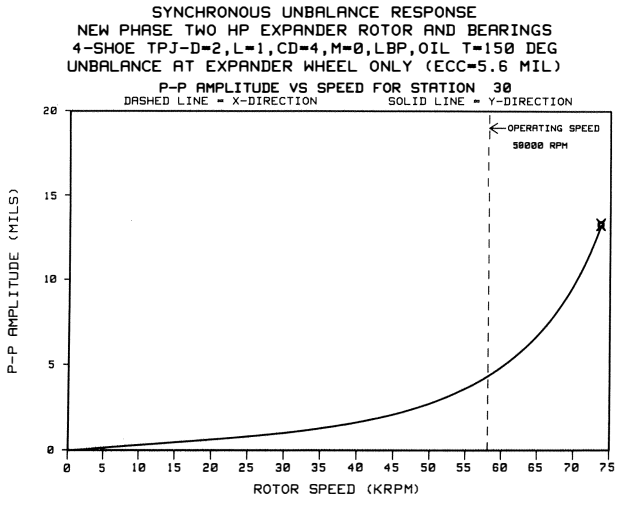

Figure 61. Synchronous Response Amplitudes (P-P Mils) vs Rotor Speed at Expander-End Impeller Location for New Phase Two HP Expander Rotor Supported on New Phase Two Bearings. Unbalance at expander-end impeller only (Eccentricity = 5.6 mils).

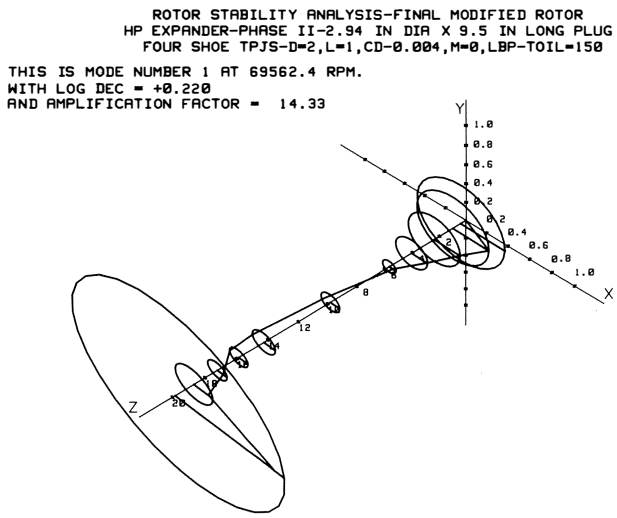

Figure 63. Third Backward Whirl Mode Shape for New Phase Two HP Expander Rotor Supported on New Phase Two Bearings. Operating Speed = 58,000 rpm. Damped Eigenvalue Frequency = 69,562 rpm. Log Decrement = +0.22.

that the original system yielded a third forward mode at 79,011 rpm with a log dec of +0.03 and a third backward mode at 66,880 rpm with a log dec of +0.07. The corresponding Phase One forward mode is 78,041 rpm with a log dec of +0.09 and the backward mode is 66,121 rpm with a log dec of +0.08.

SUMMARY AND CONCLUSIONS

This analysis has shown that the solution of turbomachinery problems can be addressed from different levels. Specifically, the

rotordynamics analysis predictive capabilities can be applied to identify several levels of retrofit. The simplest retrofit would be a "roll-in" bearing that could be immediately installed. While the first phase retrofit is in operation, a follow up analysis can be pursued on the computer model in order to explore areas of further potential improvement.

Table 15. Amplitudes (P-P Mils) and Phase Angles at 58,000 RPM for New Phase Two HP Expander Rotor Supported on New Phase Two Tilting Pad Journal Bearings. Unbalance at expander-end impeller only (Eccentricity = 5.6 Mils).

Station Number	X-Amplitude (P-P Mils)	X-Phase (Degrees)	Y-Amplitude (P-P Mils)	Y-Phase (Degrees)
1	2.7	330	2.7	330
2	2.5	329	2.5	329
3	2.3	328	2.3	328
4	2.2	328	2.2	328
5	2.0	326	2.0	326
6	1.8	325	1.8	325
7	1.6	323	1.6	323
8	1.3	320	1.3	320
9	1.2	318	1.2	318
10	0.9	311	0.9	311
11	0.6	287	0.6	287
12	0.6	281	0.6	281
13	0.5	275	0.5	275
14	0.5	255	0.5	255
15	0.7	205	0.7	205
16	1.0	184	1.0	184
17	1.2	172	1.2	172
18	1.2	159	1.2	159
19	1.2	155	1.2	155
20	1.2	154	1.2	154
21	1.2	152	1.2	152
22	1.1	135	1.1	135
23	1.0	112	1.0	112
24	1.0	97	1.0	97
25	1.1	88	1.1	88
26	1.2	79	1.2	79
27	1.3	70	1.3	70
28	2.3	43	2.3	43
29	3.5	32	3.5	32
30	4.3	28	4.3	28
31	4.7	27	4.7	27
32	5.0	26	5.0	26

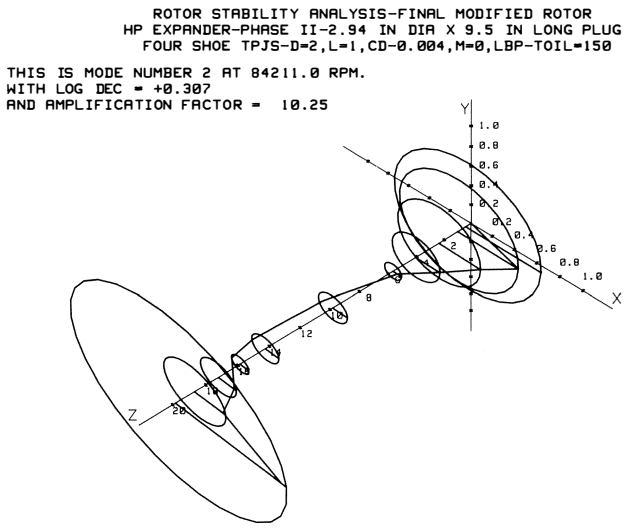

Figure 64. Third Forward Whirl Mode Shape for New Phase Two HP Expander Rotor Supported on New Phase Two Bearings. Operating Speed = 58,000 rpm. Damped Eigenvalue Frequency = 84,211 rpm. Log Decrement = +0.31.

Table 16. Rotor Stability Results for New Phase Two HP Expander Rotor Supported on New Phase Two Tilting Pad Journal Bearings. Operating Speed = 58,000 RPM.

Eigenvalue Number	Damped Frequency (RPM)	Logarithmic Decrement (DIM)	Stability Condition	Whirl Direction
1	69,562	+0.22	Stable	Backward
2	84,211	+0.31	Stable	Forward

In the case of the subject HP expander, the first improvement (Phase One) consisted of a "roll-in" set of bearings that would fit in the existing bearing housing configuration and adapt to the original rotor. While the Phase One retrofit was in operation, a backup contingency plan (Phase Two) was pursued. The purpose for the Phase Two analysis was to assess the system from a complete new redesign approach. This Phase Two option considered the potential improvements for more extensive hardware changes, which could include a complete new rotor, new bearings and even a new bearing housing, if necessary.

The following section is a summary of the original system analysis and the results of Phase One and Phase Two.

Original Rotor and Bearings

The predicted lateral rotordynamic characteristics of the HP expander in the original three lobe journal bearings can be summarized as follows:

- The synchronous unbalance response analysis predicted that an unbalance equivalent to a 5.6 mil eccentricity at the expander-end impeller could excessively load the expander-end bearing and initiate shaft-to-bearing contact. Therefore, this unbalance amount was referred to as the "worst case" assumed unbalance condition.

- The original stability analysis revealed that the first and second modes are only marginally stable. The third forward whirl mode occurs at 79,011 rpm with a log dec of +0.03. The third backward whirl mode occurs at 66,880 rpm with a log dec of +0.07. The close proximity of this sensitive backward mode frequency to the design operating speed of 57,300 rpm is not desirable, because it was possible that this mode might be excited by an unbalance-initiated rub. Therefore, it is a significant weakness in the rotor bearing system.

Phase One Bearing Redesign

The predicted lateral rotordynamic characteristics of the HP expander in the new Phase One tilt pad journal bearings can be summarized as follows:

- The new Phase One bearings significantly improve the expander unbalance response amplitudes compared to the response with the original bearings. This amplitude reduction can reduce the chances of exciting the sensitive third backward whirl mode due to a hard rub, as previously discussed.

- The rotor stability condition with the new Phase One bearings is slightly improved, compared to that with the original three-lobe bearings. However, the Phase One log decrements are still lower than desired.

- This analysis has shown that the Phase One bearing retrofit significantly improves the unbalance response of the expander rotor. This improvement should diminish the chances of experiencing a rub due to excess vibration amplitude. However, the Phase One retrofit does not eliminate the third backward whirl

mode problem. The potential for this problem to occur could be significantly reduced by increasing the log decrement and shifting the whirl frequency further away from operating speed. In order to meet these goals, a more extensive shaft and bearing redesign was required. This redesign was addressed in Phase Two as a backup contingency.

Phase Two Rotor and Bearing Redesign

The predicted lateral rotordynamic characteristics of the HP expander with the new Phase Two rotor and tilt pad journal bearings can be summarized as follows:

- The Phase Two redesign unbalance response results at the expander-end bearing are the same as the Phase One improvement. In addition, the Phase Two system predictions indicate amplitude reductions at other shaft locations.

- The Phase Two system significantly improves the rotor stability condition compared to the original and Phase One systems.

Analytically, the Phase Two redesign goals were met. However, due to the success of the Phase One retrofit, the Phase Two hardware retrofit never was required.

Closing Comments

The expanders ran very successfully on the Phase One bearing redesign for over four and one-half years. During this time there were no bearing failures, even though there was still some evidence of minor erosion due to solid particles in the gas stream, which could negatively-affect the rotor unbalance condition. During this successful operating time frame, there were also numerous occasions when process and/or operational-related problems occurred, that from past experience, would have caused bearing failures with the original bearing design. On several occasions the HP expander was unintentionally tripped on overspeed at 63,500 rpm without any detrimental effects. This success was a milestone of significant proportions. As a direct result of the Phase One bearing retrofit, the mechanical reliability of the HP expander was at an all time high and was no longer a concern for plant operations. It was equally important that the increased capacity resulted from being able to reliably operate the expander at the original design speed with very low shaft vibration and normal bearing temperature levels.

After the long period of successful operation with the Phase One modification, it was desired to upgrade the expander units for increased throughput. A complete new expander design was purchased to meet these requirements. Some of the Phase Two redesign improvement recommendations can be seen in the new OEM units, which lends confidence that Phase Two was on the right track.

REFERENCES

1. Salamone, D. J., "Journal Bearing Design Types and Their Applications to Turbomachinery," *Proceedings of the Thirteenth Turbomachinery Symposium,* Turbomachinery Laboratories, Department of Mechanical Engineering, Texas A&M University, College Station, Texas, pp. 179-188 (1984).
2. Lund, J. W., and Orcutt, F. K., "Calculations and Experiments on the Unbalance Response of a Flexible Rotor," Journal of Engineering for Industry, Trans. ASME, Series B, 89 (4), pp. 785-796 (November 1967).
3. Salamone, D. J. and Gunter E. J., "Effects of Shaft Warp and Disk Skew on the Synchronous Unbalance Response of a Multimass Flexible Rotor in Fluid Film Bearings," Topics in Fluid Film Bearing and Rotor Bearing System Design and Optimization, ASME Book No. 100118 (1978).
4. Barrett, L. E., Gunter, E. J., and Allaire, P. E., "Optimum Bearing and Support Damping for Unbalance Response and Stability of Rotating Machinery," Journal of Engineering for Power, Trans. ASME, (100) 1, pp. 89-94 (1978).
5. Gunter, E. J., "Dynamic Stability of Rotor-Bearing Systems," NASA SP-113, Office of Technical Utilization, U.S. Government Printing Office, Washington, D.C. (1966).
6. Lund, J. W., "Stability and Damped Critical Speeds of a Flexible Rotor in Fluid Film Bearings," Journal of Engineering for Industry, Trans. ASME, Series B, 96 (2), pp. 509-517 (May 1974).

BIBLIOGRAPHY

Bloch, H.P., *Improving Machinery Reliability,* Houston, Texas: Gulf Publishing Company (1982).

Bloch H.P. and Geitner, F.K., *An Introduction to Machinery Reliability Assessment,* Houston, Texas: Gulf Publishing Company (1990).

Falkenhagen, G.L., Gunter, E.J., and Schuller, F.T.,"Stability and Transient Motion of a Vertical Three-Lobe Bearing System," Journal of Engineering for Industry, Trans. ASME, Series B, 94 (2), pp. 665-677 (1972).

Falkenhagen, G.L., "Stability and Transient Motion of a Hydrodynamic Horizontal Three-Lobe Bearing System," The Shock and Vibration Digest, 7 (5) (1975).

Jackson, C. J., *The Practical Vibration Primer,* Houston, Texas: Gulf Publishing Company, (1979).

Kirk, R. G., "The Influence of Manufacturing Tolerance on Multi-Lobe Bearing Performance in Turbomachinery," Topics in Fluid Film Bearing and Rotor Bearing System Design and Optimization, ASME Book No. 100118, pp. 108-129 (1978).

Lund, J. W., "Spring and Damping Coefficients for the Tilting-Pad Journal Bearing," Trans. ASLE, 7 (4), pp. 342-352 (1964).

Lund, J.W., "Rotor-Bearing Dynamics Design Technology, Part VII: The Three-Lobe Bearing and Floating Ring Bearing," Mechanical Technology Incorporated, Technical Report No. AFAPL-TR-64-45 (1968).

Mitchell, J. S., *Machinery Analysis and Monitoring,* Tulsa, Oklahoma: PennWell Publishing Company, (1981).

Nicholas, J.C., Gunter, E.J., and Allaire, P.E., "Stiffness and Damping Coefficients for the Five Pad Tilting Pad Bearing," Trans. ASLE, 22(2), pp. 113-124 (1979).

Pinkus, O., "Analysis and Characteristics of the Three Lobe Bearing," Journal of Basic Engineering, Trans. ASME, pp. 49-55 (1959).

Salamone, D. J., "Introduction to Hydrodynamic Journal Bearings," Vibration Institute Minicourse Notes—Machinery Vibration Monitoring and Analysis, The Vibration Institute, Clarendon Hills, Illinois, pp. 41-56 (1985).